

Novel moduli space in modular flavor models : a case study for modular T' seesaw model with hidden $SU(2)$ gauge symmetry

Keiya Ishiguro¹, Takaaki Nomura², Hiroshi Okada³, Yuta Orikasa⁴, Hajime Otsuka³

¹Graduate University for Advanced Studies (Sokendai), 1-1 Oho, Tsukuba, Ibaraki 305-0801, Japan

²College of Physics, Sichuan University, Chengdu 610065, China

³Department of Physics, Kyushu University, 744 Motoooka, Nishi-ku, Fukuoka 819-0395, Japan

⁴Institute of Experimental and Applied Physics, Czech Technical University in Prague, Husova 240/5, 110 00 Prague 1, Czech Republic

E-mail: ishigu@post.kek.jp, nomura@scu.edu.cn,
okada.hiroshi@phys.kyushu-u.ac.jp, Yuta.Orikasa@utef.cvut.cz,
otsuka.hajime@phys.kyushu-u.ac.jp

ABSTRACT: We study flavor phenomenologies in a basis of a double covering of modular A_4 group with a hidden $SU(2)$ symmetry, in which we work on regions at nearby two fixed points and three special points. These special points of $SL(2, \mathbb{Z})$ moduli space are statistically favored in flux compactifications of Type IIB string theory. Neutrino masses are approximately obtained by using the seesaw mechanism due to our two additional symmetries. We perform chi square numerical analysis for each of the fixed/special points in the normal and inverted hierarchies and demonstrate predictions for each case. Then, we briefly discuss the possible signature of hidden gauge bosons at collider experiments from the hidden $SU(2)$ symmetry.

Contents

1	Introduction	1
2	Novel moduli values from top-down approach	4
3	Model setup	5
4	Numerical analysis	9
4.1	NH	9
4.1.1	$\tau = i$	10
4.1.2	$\tau = \omega$	11
4.1.3	$\tau = -\frac{1}{2} + \frac{\sqrt{15}}{2}i$	12
4.1.4	$\tau = \sqrt{3}i$	13
4.1.5	$\tau = -\frac{1}{4} + \frac{\sqrt{15}}{4}i$	14
4.2	IH	14
4.2.1	$\tau = i$	15
4.2.2	$\tau = \omega$	16
4.2.3	$\tau = -\frac{1}{2} + \frac{\sqrt{15}}{2}i$	17
4.2.4	$\tau = \sqrt{3}i$	18
4.2.5	$\tau = -\frac{1}{4} + \frac{\sqrt{15}}{4}i$	19
4.3	Multiple dark gauge bosons in the model	19
5	Summary and discussions	21

1 Introduction

One of the main issues in the Standard Model (SM) is to explain the flavor structure of quarks and leptons by some mechanisms. Among many possibilities, a flavor symmetry plays an important role in understanding the hierarchical masses and mixing angles of the SM fermions.

In models with flavor symmetries, Yukawa couplings are considered as a singlet or a non-trivial representation under a flavor symmetry. The former scenario was known to be the traditional approach to understand the flavor structure of quarks and leptons¹, but the latter scenario is more attractive and natural from the viewpoint of ultraviolet physics [4]. Indeed, in the higher-dimensional theory such as the string theory, the Yukawa couplings are given by the overlap integral of matter wavefunctions once quarks and leptons live in the bulk space of the extra-dimensional space. It indicates that the Yukawa couplings will be controlled by a geometric symmetry of the extra-dimensional space such as the (finite part

¹See for more details, e.g., Refs. [1-3].

of) $SL(2, \mathbb{Z})$ modular symmetry in the single modulus and $Sp(2g, \mathbb{Z})$ modular symmetry in multi moduli case. The explicit model buildings have been performed in heterotic string on toroidal orbifolds [5–10] and Calabi-Yau threefolds [10, 11], and Type IIB magnetized D-branes [4, 12–16].

Since the Yukawa couplings depend on the so-called moduli fields, the moduli vacuum expectation values (VEVs) are important to predict the flavor pattern of quarks and leptons. In particular, residual symmetries in the $SL(2, \mathbb{Z})$ moduli space of τ exist at some particular points of moduli space, called fixed points, such as $\tau = i, \omega, i\infty$ with $\omega = \frac{-1+i\sqrt{3}}{2}$, corresponding to $\mathbb{Z}_2, \mathbb{Z}_3$ and \mathbb{Z}_2 symmetries, which was phenomenologically applied in the lepton sector [17–28]. Remarkably, the $SL(2, \mathbb{Z})$ modular symmetry breaking was performed in [29], and moduli VEVs are predicted by a top-down approach, e.g., Type IIB string compactifications with background fluxes [30], and the deviation of the moduli field from the fixed points was achieved in Ref. [31]. In the top-down approach of Ref. [30], distributions of moduli fields from a finite number of string flux vacua suggest us that the moduli VEVs are statistically favored at the other special points such as $\tau = \frac{-1+i\sqrt{15}}{2}, \sqrt{3}i, \frac{-1+i\sqrt{15}}{4}$ in addition to the fixed points $\tau = i, \omega$. Note that these points are not protected by a certain symmetry.

In the bottom-up approach, there is no guiding principle to pick up certain moduli VEVs from the $SL(2, \mathbb{Z})$ moduli space. In this paper, we discuss the phenomenological aspects of these special moduli values $\tau = i, \omega, \frac{-1+i\sqrt{15}}{2}, \sqrt{3}i, \frac{-1+i\sqrt{15}}{4}$, predicted by the top-down approach. Note that $\tau = i\infty$ will be excluded by the cancellation of D-brane charges, or in other words, we require the infinite value of background flux quanta to approach $\tau = i\infty$. For illustrative purposes, we focus on the lepton sector in the seesaw model with a double covering of modular A_4 symmetry; T' , and hidden $SU(2)$ gauge symmetry. The hidden symmetry is useful to construct the seesaw model by discriminating heavy neutral fermions that typically appear in seesaw models in the framework of modular symmetry with an ordinal modular weight assignments [32]. The additional symmetries naturally appear in the low-energy effective action of the string theory². Even though the minimum flavor symmetry including an irreducible triplet is A_4 symmetry and a vast amount of literature has been appeared in refs. [18, 21, 23–25, 33–60], in this paper, we apply its double covering group because of following reasons. The first one is that this group possesses an irreducible doublet that could be identified as a representation for heavier Majorana fermions. Therefore, the active neutrino mass matrix is minimally realized by rank two matrix. The second one is that T' allows us to use an odd number of modular weights for Yukawa couplings and different types of mass matrices could be obtained compared to the one with A_4 .

In this paper, instead of hidden $U(1)$, we adopt the non-Abelian gauge symmetry $SU(2)$ which also appears in the low-energy effective action of the string theory.³ In a typical interpretation of "hidden symmetry", we expect that the $SU(2)$ symmetry has to (almost) be separated from the SM sector due to the structure of $SU(2)$. It suggests that

²See, Refs. [5, 6], for the realization of the modular T' symmetry.

³See, e.g., Ref. [61], for the statistical approach of D-brane model building on toroidal orientifolds and Ref. [62] for $SO(32)$ heterotic model building in general Calabi-Yau compactifications.

there exist no interactions between these two sectors or the interactions has to be very small. However, if we introduce a hidden $U(1)$ symmetry, we have no way to eliminate the kinetic mixing between the SM and hidden sector except for assuming the mixing to be enough small by hand. In case of hidden non-Abelian symmetry, the mixing would not be appeared without an intermediate sector that has both the SM and hidden charge. The mixing can appear with the intermediate sector at a tree level or at a loop level [63, 64]. Moreover, a remnant symmetry after spontaneous symmetry breaking of $SU(2)$ controls the stability of dark matter even though we do not discuss here. The unbroken symmetry can be naturally preserved compared to the Abelian symmetry in which the $U(1)$ charge has to satisfy some artificial tuning [65]. In fact, various applications of the hidden $SU(2)$ gauge symmetries have been studied in articles, e.g., a remaining \mathbb{Z}_2 symmetry in ref. [66], $\mathbb{Z}_3(\mathbb{Z}_4)$ symmetry with a quadruplet(quintet) in Ref. [67–69], $\mathbb{Z}_2 \times \mathbb{Z}'_2$ symmetry [70], a custodial symmetry in refs. [71, 72], an unbroken $U(1)$ from $SU(2)$ in refs. [73–75], a model adding hidden $U(1)_H$ [76] and a model with classical scale invariance [77]. It is then challenging and interesting to consider neutrino mass generation with hidden $SU(2)$. Hidden $SU(2)$ can also be applied to discriminate heavy neutral fermions from the SM sector, and intermediate sector inducing mixing between hidden and the SM sector also play a role in generating neutrino mass. In addition one finds that we need at least two generations of heavy neutral fermion if it is $SU(2)$ doublet in order to cancel the anomaly [78]. This minimal two generations of hidden heavy doublet can be organized into T' doublet and thus we have good compatibility between hidden $SU(2)$ and T' . In the model of this work, hidden $SU(2)_H$ symmetry is spontaneously broken by VEVs of scalar fields including $SU(2)_L \times SU(2)_H$ bidoublets. Then Majorana fermions in the hidden sector can mix with active neutrinos in the SM sector inducing the type-I like seesaw mechanism [79–81]. Furthermore we would have interesting phenomenology from hidden vector bosons in the model. In our scenario two hidden vector bosons from the $SU(2)_H$ mix with the SM neutral Z boson since $SU(2)_L \times SU(2)_H$ bidoublet scalar fields get VEVs. On the other hand one hidden vector boson does not directly mix with the SM gauge boson. Thus we have two dark photons like vector bosons and one vector boson which does not couple to the SM particles. The latter one would be long lived one and could provide a distinguishable signature at the collider experiments. We discuss these hidden vector bosons and the possibility of their collider phenomenology briefly.

The remaining section is organized as follows. In Sect.2, we review two fixed points and three special points which are known as stable vacua and discuss their origin based on four-dimensional effective action of Type IIB string theory. In Sect.3, we show our model set up to generate the seesaw model in a framework of modular T' and hidden gauge $SU(2)$ symmetries. Then, we demonstrate numerical analyses and display our predictions in each of the five points that we have discussed in Sect. 2. Then, we discuss the possibility of testability via colliders in the multiple dark gauge boson sector. Finally, we give our summary and discussions.

2 Novel moduli values from top-down approach

In this section, we briefly review the distribution of moduli fields on the basis of four-dimensional effective action of Type IIB string theory. (For more details, see, e.g., Refs. [82–84].) Since the modulus field τ determines the fermion mass hierarchies and mixing angles in modular flavor models, it is important to fix the vacuum expectation value by some mechanisms. In higher-dimensional theories, background p -form fluxes in compact extra-dimensional spaces will induce the potential of moduli fields. Indeed, in Type IIB flux compactifications, the background three-form fluxes generate the four-dimensional superpotential [85]:

$$W(S, \tau) = \int G_3 \wedge \Omega, \quad (2.1)$$

where $G_3 = F_3 - SH_3$ is defined as a linear combination of Ramond-Ramond three-form F_3 and Neveu-Schwarz three-form H_3 , and Ω is a holomorphic three-form of the internal six-dimensional space as a function of a certain complex structure modulus τ . It results in the potential of axio-dilaton S and complex structure modulus τ . Specifically, we focus on $T^6/(\mathbb{Z}_2 \times \mathbb{Z}_2)$ geometry which incorporating the overall $SL(2, \mathbb{Z})_\tau$ modular symmetry used in modular flavor models.

On $T^6/(\mathbb{Z}_2 \times \mathbb{Z}_2)$ geometry, the superpotential with the modular weight 3 is of the form:

$$W = a^0 \tau^3 - 3a\tau^2 - 3b\tau - b_0 - S(c^0 \tau^3 - 3c\tau^2 - 3d\tau - d_0), \quad (2.2)$$

where the coefficients of the modulus τ represent a flux quanta. Together with the kinetic terms of S and τ written in the Kähler potential:

$$K = -\ln(-i(S - \bar{S})) - 3\ln(i(\tau - \bar{\tau})) - 2\ln \mathcal{V}, \quad (2.3)$$

one can check the $PSL(2, \mathbb{Z})_\tau$ and $PSL(2, \mathbb{Z})_S$ modular symmetries following Refs. [30, 86]. Throughout this paper, we do not study the stabilization of volume moduli \mathcal{V} , but it is possible to stabilize them following the prescription of Ref. [31] in the context of modular flavor models. The moduli S and τ can be stabilized at supersymmetric minima:

$$\partial_S W = \partial_\tau W = W = 0, \quad (2.4)$$

leading to the following vacuum expectation value of moduli fields:

$$S = \frac{r\tau + s}{u\tau + v}, \quad \tau = \begin{cases} \frac{-m + \sqrt{m^2 - 4ln}}{2l} & (l, n > 0) \\ \frac{-m - \sqrt{m^2 - 4ln}}{2l} & (l, n < 0) \end{cases}. \quad (2.5)$$

Here, we redefine the flux quanta

$$\begin{aligned} rl = a^0, \quad rm + sl = -3a, \quad rn + sm = -3b, \quad sn = -b_0, \\ ul = c^0, \quad um + vl = -3c, \quad un + vm = -3d, \quad vn = -d_0. \end{aligned} \quad (2.6)$$

It was known that fixed points of $SL(2, \mathbb{Z})_\tau$ moduli space $\tau = \omega, i$ with $\omega = (-1 + i\sqrt{3})/2$ are statistically favored in the flux landscape. Note that a region around the remaining fixed point $\tau = i\infty$ cannot be realized in flux compactifications due to the fact that the D3-brane charge induced by three-form flux quanta:

$$N_{\text{flux}} = \int H_3 \wedge F_3 = c^0 b_0 - d_0 a^0 + 3(cb - da) \quad (2.7)$$

should be canceled in a compact space, and the value is upper bounded by D-brane and O-plane charges in string compactifications. Remarkably, the flux landscape also prefer other special points of $SL(2, \mathbb{Z})$ moduli space:

$$\tau = \frac{-1 + i\sqrt{15}}{2}, \sqrt{3}i, \frac{-1 + i\sqrt{15}}{4}, \dots, \quad (2.8)$$

as shown in Table 1. Here, we list the stable vacua, up to 5, in the descending order of the probability by setting a maximum value of N_{flux} , that is, $N_{\text{flux}}^{\text{max}} = 192 \times 10$. Although the value of probabilities depends on $N_{\text{flux}}^{\text{max}}$, the statistical behavior is similar for other $N_{\text{flux}}^{\text{max}}$. In this respect, it is interesting to figure out a phenomenological aspect of these novel points in the moduli space. In the following sections, we deal with a modular T' seesaw model with hidden $SU(2)$ gauge symmetry as a case study.

$(\text{Re } \tau, \text{Im } \tau)$	$(-\frac{1}{2}, \frac{\sqrt{3}}{2})$	$(0, \sqrt{3})$	$(-\frac{1}{2}, \frac{\sqrt{15}}{2})$	$(-\frac{1}{4}, \frac{\sqrt{15}}{4})$	$(0, 1)$
Probability (%)	62.3	7.55	7.55	7.55	5.66

Table 1. Probabilities of the stable vacua as functions of $(\text{Re } \tau, \text{Im } \tau)$ in the finite number of flux vacua [30].

3 Model setup

	\hat{L}	$(\hat{e}^c, \hat{\mu}^c, \hat{\tau}^c)$	$\hat{\Sigma}^c$	$\hat{\Phi}_1$	$\hat{\Phi}_2$	\hat{H}_X	\hat{H}_u	\hat{H}_d	$\hat{\Delta}$
$SU(2)_H$	1	1	2	2	2	2	1	1	3
$SU(2)_L$	2	1	1	2	2	1	2	2	1
$U(1)_Y$	$-\frac{1}{2}$	1	0	$\frac{1}{2}$	$-\frac{1}{2}$	0	$\frac{1}{2}$	$-\frac{1}{2}$	0
T'	3	(1, 1', 1'')	2	1	1	2	1	1	1
$-k_I$	-2	$(-4, -4, -8)$	-1	-4	-4	-1	0	0	-4

Table 2. Charge assignments of matter superfields under $SU(2)_H \times SU(2)_L \times U(1)_Y \times T'$, where all of them are singlet under $SU(3)_C$ and R-parity is assigned; $\hat{L}, \hat{e}, \hat{\Sigma}^c$ for minus and the other superfields for plus. $\hat{\Sigma}^c$ has two generations that are organized in T' doublet in order to cancel the anomaly for $SU(2)_H$ [78].

In this section we formulate our model in which we introduce hidden $SU(2)_H$ gauge symmetry and modular T' symmetry. The matter superfields in Lepton and scalar sector are summarized in Table 2 with their charge assignment under $SU(2)_H \times SU(2)_L \times U(1)_Y \times T'$ and modular weight where scalar sector means the scalar components in the sector

develops VEVs. In the scalar sector, we introduce $SU(2)_H$ doublet H_X and $\Phi_{1,2}$ where the former one is SM gauge singlet and the latter one is also $SU(2)_L$ doublet with $U(1)_Y$ charge 1/2. In our scenario all these scalar fields develop VEVs inducing spontaneous symmetry breaking. The scalar components in the superfields are written as follows:

$$H_u = \begin{pmatrix} h_u^+ \\ \frac{1}{\sqrt{2}}(v_u + h_u + ia_u) \end{pmatrix}, \quad H_d = \begin{pmatrix} \frac{1}{\sqrt{2}}(v_d + h_d + ia_d) \\ h_d^- \end{pmatrix}, \quad (3.1)$$

$$H_X = \begin{pmatrix} \eta_{1/2} \\ \frac{1}{\sqrt{2}}(v_X + p_{-1/2} + iq_{-1/2}) \end{pmatrix}, \quad (3.2)$$

$$\Phi_1 = \begin{pmatrix} \phi_{1/2}^+ & \phi_{-1/2}^+ \\ \frac{1}{\sqrt{2}}(\kappa + r_{1/2} + ia_{1/2}) & \frac{1}{\sqrt{2}}(\kappa' + r'_{-1/2} + ia'_{-1/2}) \end{pmatrix}, \quad (3.3)$$

$$\Phi_2 = \begin{pmatrix} \frac{1}{\sqrt{2}}(\zeta + q_{1/2} + ib_{1/2}) & \frac{1}{\sqrt{2}}(\zeta' + q'_{-1/2} + ib'_{-1/2}) \\ \varphi_{1/2}^- & \varphi_{-1/2}^- \end{pmatrix}, \quad (3.4)$$

$$\Delta = \begin{pmatrix} \frac{1}{\sqrt{2}}\sigma_0 & v_+ + \sigma_{+1} \\ v_- + \sigma_{-1} & -\frac{1}{\sqrt{2}}\sigma_0 \end{pmatrix}, \quad (3.5)$$

where $v_{u,d,X}$ and $\kappa, \kappa', \zeta, \zeta'$ are VEVs for corresponding fields, and the upper number indices are electric charges and the lower ones are hidden charges. Notice here that fields have zero charges without number symbols, and they have plus charges under R-parity. In addition, $SU(2)_H$ doublet fermions Σ^c are introduced which is taken as right-handed and SM gauge singlet. We write the fermionic particles in the superfield Σ^c with their components as

$$\Sigma_i^c = \begin{pmatrix} N_{1/2}^{ic} \\ n_{-1/2}^{ic} \end{pmatrix}, \quad (3.6)$$

where both component fields are electrically neutral, and the field has to have the even number of generations for guaranteeing the theory to be anomaly free associated with $SU(2)_H$; $i = 1, 2$ [78]. In the model, we fix two generations to this field as minimal choice and they are organized as T' doublet. $\hat{\Sigma}^c$ has minus R-parity charge as well as SM leptons. Then, the invariant superpotential under these symmetries is given by

$$\begin{aligned} W = & a_\ell [Y_{3_1}^{(6)} e^c \hat{L} \cdot \hat{H}_d] + a'_\ell [Y_{3_2}^{(6)} e^c \hat{L} \cdot \hat{H}_d] \\ & + b_\ell [Y_{3_1}^{(6)} \mu^c \hat{L} \cdot \hat{H}_d] + b'_\ell [Y_{3_2}^{(6)} \mu^c \hat{L} \cdot \hat{H}_d] \\ & + c_\ell [Y_{3_1}^{(10)} \tau^c \hat{L} \cdot \hat{H}_d] + c'_\ell [Y_{3_2}^{(10)} \tau^c \hat{L} \cdot \hat{H}_d] + c''_\ell [Y_{3_3}^{(10)} \tau^c \hat{L} \cdot \hat{H}_d] \\ & + a_\nu [Y_{2_1}^{(7)} \hat{L} \cdot \hat{\Phi}_1 \cdot \hat{\Sigma}^c] + a'_\nu [Y_{2_2}^{(7)} \hat{L} \cdot \hat{\Phi}_1 \cdot \hat{\Sigma}^c] \\ & + b_\nu [Y_{2_1}^{(7)} \hat{L} \cdot \hat{\Phi}_1 \cdot \hat{\Sigma}^c] + c_\nu [Y_{2_2}^{(7)} \hat{L} \cdot \hat{\Phi}_1 \cdot \hat{\Sigma}^c] \\ & + \mu_H \hat{H}_u \cdot \hat{H}_d + \kappa_{\Sigma_1} Y_{3_1}^{(6)} \hat{\Sigma}^c \cdot \hat{\Delta} \hat{\Sigma}^c + \kappa_{\Sigma_2} Y_{3_2}^{(6)} \hat{\Sigma}^c \cdot \hat{\Delta} \hat{\Sigma}^c + \mu_\Delta \hat{\Delta} \hat{\Delta} + \mu_\Phi \hat{\Phi}_1 \cdot \hat{\Phi}_2 \\ & + a \hat{\Phi}_1 \hat{\Delta} \cdot \hat{\Phi}_2 + b \hat{H}_d \cdot \hat{\Phi}_1 \cdot \hat{H}_X + c \hat{H}_u \cdot \hat{\Phi}_2 \cdot \hat{H}_X + d \hat{H}_X \cdot \hat{\Delta} \cdot \hat{H}_X, \end{aligned} \quad (3.7)$$

where $\cdot \equiv i\sigma_2$ is the second Pauli matrix, $[\dots]$ represents the true singlet under modular T' symmetry, and bare mass term $\hat{\Sigma}^c \cdot \hat{\Sigma}^c$ vanishes. Note here that μ_Σ should be anti-symmetric matrix due to anti-symmetric contraction of $SU(2)_H$ indices in the term. It

suggests that μ_Σ reduces the matrix rank by one, and we cannot formulate the active neutrino mass matrix. Thus, we introduce $\hat{\Delta}$ that leads to the term κ_Σ as we will see later. The bi-doublet plays a role in inducing the Dirac mass terms between active neutrino and hidden Majorana fermions that are also needed to construct the neutrino mass matrix. The explicit forms of modular forms are summarized in the appendix. We then obtain mass matrices from terms in the superpotential by expanding them using formulas for products of T' representations.

In the model charged lepton mass matrix is obtained from first 7 terms in the superpotential after H_d developing its VEV. The mass matrix is explicitly written by

$$M_\ell = \frac{v_d}{\sqrt{2}} \begin{pmatrix} a_\ell & 0 & 0 \\ 0 & b_\ell & 0 \\ 0 & 0 & c_\ell \end{pmatrix} \times \begin{pmatrix} y_1^{(6)} + \epsilon_e y_1'^{(6)} & y_3^{(6)} + \epsilon_e y_3^{(6)} & y_2^{(6)} + \epsilon_e y_2'^{(6)} \\ y_3^{(6)} + \epsilon_\mu y_1'^{(6)} & y_2^{(6)} + \epsilon_\mu y_2'^{(6)} & y_1^{(6)} + \epsilon_\mu y_1'^{(6)} \\ y_2^{(6)} + \epsilon_\tau y_2''^{(10)} + \epsilon'_\tau y_2''^{(10)} & y_1^{(6)} + \epsilon_\tau y_1'^{(10)} + \epsilon'_\tau y_1''^{(10)} & y_3^{(6)} + \epsilon_\tau y_3'^{(10)} + \epsilon'_\tau y_3''^{(10)} \end{pmatrix}, \quad (3.8)$$

where $\{\epsilon_e, \epsilon_\mu, \epsilon_\tau, \epsilon'_\tau\} = \{a'_\ell/a_\ell, b'_\ell/b_\ell, c'_\ell/c_\ell, c''_\ell/c_\ell\}$. We diagonalize the matrix to obtain the charged-lepton mass eigenvalues as $\text{diag}(|m_e|^2, |m_\mu|^2, |m_\tau|^2) \equiv V_{eL}^\dagger m_\ell^\dagger m_\ell V_{eL}$ where V_{eL} is a unitary matrix. In our numerical analysis we fix three input parameters $\{a_\ell, b_\ell, c_\ell\}$ by solving following relations:

$$\text{Tr}[m_\ell m_\ell^\dagger] = |m_e|^2 + |m_\mu|^2 + |m_\tau|^2, \quad (3.9)$$

$$\text{Det}[m_\ell m_\ell^\dagger] = |m_e|^2 |m_\mu|^2 |m_\tau|^2, \quad (3.10)$$

$$(\text{Tr}[m_\ell m_\ell^\dagger])^2 - \text{Tr}[(m_\ell m_\ell^\dagger)^2] = 2(|m_e|^2 |m_\mu|^2 + |m_\mu|^2 |m_\tau|^2 + |m_e|^2 |m_\tau|^2). \quad (3.11)$$

Here, we apply experimentally measured charged-lepton masses summarized in PDG [87].

After spontaneous symmetry breaking, we obtain a mass matrix for neutral fermion including the SM neutrino such that

$$M = \begin{pmatrix} \mathbf{0}_{3 \times 3} & M_{\nu n} & M_{\nu N} \\ M_{\nu n}^T & M_n & \mathbf{0}_{2 \times 2} \\ M_{\nu N}^T & \mathbf{0}_{2 \times 2} & M_N \end{pmatrix} + (\text{transposed}), \quad (3.12)$$

where the basis is $[\nu, n_{-1/2}^c, N_{-1/2}^c]$. The element $M_{\nu n(\nu N)}$ is 3×2 matrix that is obtained from terms with coefficient $\{a_\nu, a'_\nu, b_\nu, c_\nu\}$ in superpotential after bidoublet Φ_1 develops its VEV. Explicit form of elements in $M_{\nu n(\nu N)}$ are written by

$$M_{\nu n[\nu N]} = \frac{\kappa[\kappa']}{\sqrt{2}} \begin{pmatrix} \sqrt{2} b_\nu e^{\frac{5\pi}{12}i} f_1'^{(7)} - c_\nu f_2''^{(7)} & \sqrt{2} e^{\frac{7\pi}{12}i} (a_\nu f_2^{(7)} + a'_\nu g_2^{(7)}) - c_\nu f_1''^{(7)} \\ \sqrt{2} e^{\frac{5\pi}{12}i} (a_\nu f_1^{(7)} + a'_\nu g_1^{(7)}) - b_\nu f_2''^{(7)} & -b_\nu f_1'^{(7)} + \sqrt{2} e^{\frac{7\pi}{12}i} c_\nu f_2''^{(7)} \\ -a_\nu f_2^{(7)} - a'_\nu g_2^{(7)} + \sqrt{2} c_\nu e^{\frac{5\pi}{12}i} f_1''^{(7)} & -a_\nu f_1^{(7)} - a'_\nu g_1^{(7)} + \sqrt{2} b_\nu e^{\frac{7\pi}{12}i} f_2'^{(7)} \end{pmatrix} \\ \equiv \frac{\kappa[\kappa']}{\sqrt{2}} \tilde{M}_{\nu n}. \quad (3.13)$$

The 2×2 matrices M_n and M_N are obtained from the terms with $\{\kappa_{\Sigma_1}, \kappa_{\Sigma_2}\}$ coefficient in the superpotential after triplet Δ developing a VEV. We can explicitly write them such that

$$M_{N[n]} = v_-[-v_+] \begin{pmatrix} \kappa_{\Sigma_1} y_2^{(6)} + \kappa_{\Sigma_2} y_2'^{(6)} & \frac{1}{\sqrt{2}} e^{\frac{7\pi}{12}i} (\kappa_{\Sigma_1} y_3^{(6)} + \kappa_{\Sigma_2} y_3'^{(6)}) \\ \frac{1}{\sqrt{2}} e^{\frac{7\pi}{12}i} (\kappa_{\Sigma_1} y_3^{(6)} + \kappa_{\Sigma_2} y_3'^{(6)}) & e^{\frac{\pi}{6}i} (\kappa_{\Sigma_1} y_1^{(6)} + \kappa_{\Sigma_2} y_1'^{(6)}) \end{pmatrix} \\ \equiv v_-[-v_+] \tilde{M}_n. \quad (3.14)$$

The active neutrino mass in the mode is given by type-I seesaw like with both Majorana fermion n and N such that

$$m_\nu \simeq -M_{\nu n} M_n^{-1} M_{\nu n}^T - M_{\nu N} M_N^{-1} M_{\nu N}^T, \\ \left(\frac{\kappa^2}{2v_+} - \frac{\kappa'^2}{2v_-} \right) \tilde{M}_{\nu n} \tilde{M}_n^{-1} \tilde{M}_{\nu n}^T \equiv \epsilon \tilde{m}_\nu, \quad (3.15)$$

where $\epsilon \equiv \frac{\kappa^2}{2v_+} - \frac{\kappa'^2}{2v_-}$. m_ν is diagonalized by a unitary matrix V_ν ; $D_\nu = |\epsilon| \tilde{D}_\nu = V_\nu^T m_\nu V_\nu = |\epsilon| V_\nu^T \tilde{m}_\nu V_\nu$. Then $|\epsilon|$ is determined by

$$(\text{NH}) : |\epsilon|^2 = \frac{|\Delta m_{\text{atm}}^2|}{\tilde{D}_{\nu_3}^2 - \tilde{D}_{\nu_1}^2}, \quad (\text{IH}) : |\epsilon|^2 = \frac{|\Delta m_{\text{atm}}^2|}{\tilde{D}_{\nu_2}^2 - \tilde{D}_{\nu_3}^2}, \quad (3.16)$$

where Δm_{atm}^2 is the atmospheric neutrino mass square difference. (NH) and (IH) respectively represent the normal hierarchy and the inverted hierarchy. Then, the solar mass square difference is written in terms of $|\epsilon|$ as follows:

$$\Delta m_{\text{sol}}^2 = |\epsilon|^2 (\tilde{D}_{\nu_2}^2 - \tilde{D}_{\nu_1}^2), \quad (3.17)$$

which is compared to the observed value in our numerical analysis. The observed mixing matrix is defined by $U = V_{eL}^\dagger V_\nu$ [88], where it is parametrized by the following three mixing angles, one CP violating Dirac phase δ_{CP} , and one Majorana phase α_{21} :

$$U = \begin{pmatrix} c_{12}c_{13} & s_{12}c_{13} & s_{13}e^{-i\delta_{\text{CP}}} \\ -s_{12}c_{23} - c_{12}s_{23}s_{13}e^{i\delta_{\text{CP}}} & c_{12}c_{23} - s_{12}s_{23}s_{13}e^{i\delta_{\text{CP}}} & s_{23}c_{13} \\ s_{12}s_{23} - c_{12}c_{23}s_{13}e^{i\delta_{\text{CP}}} & -c_{12}s_{23} - s_{12}c_{23}s_{13}e^{i\delta_{\text{CP}}} & c_{23}c_{13} \end{pmatrix} \begin{pmatrix} 1 & 0 & 0 \\ 0 & e^{i\frac{\alpha_{21}}{2}} & 0 \\ 0 & 0 & 1 \end{pmatrix}, \quad (3.18)$$

where c_{ij} and s_{ij} ($i, j = 1, 2, 3; i < j$) stand for $\cos \theta_{ij}$ and $\sin \theta_{ij}$, respectively. Each of the mixings is given in terms of the component of U as follows:

$$\sin^2 \theta_{13} = |U_{e3}|^2, \quad \sin^2 \theta_{23} = \frac{|U_{\mu 3}|^2}{1 - |U_{e3}|^2}, \quad \sin^2 \theta_{12} = \frac{|U_{e2}|^2}{1 - |U_{e3}|^2}, \quad (3.19)$$

and the Majorana phase α_{21} and Dirac phase δ_{CP} are found in terms of the following relations:

$$\text{Im}[U_{e1}^* U_{e2}] = c_{12}s_{12}c_{13}^2 \sin\left(\frac{\alpha_{21}}{2}\right), \quad \text{Im}[U_{e1}^* U_{e3}] = -c_{12}s_{13}c_{13} \sin \delta_{\text{CP}}, \quad (3.20)$$

$$\text{Re}[U_{e1}^* U_{e2}] = c_{12}s_{12}c_{13}^2 \cos\left(\frac{\alpha_{21}}{2}\right), \quad \text{Re}[U_{e1}^* U_{e3}] = c_{12}s_{13}c_{13} \cos \delta_{\text{CP}}, \quad (3.21)$$

where $\alpha_{21}/2$, δ_{CP} are subtracted from π , when $\cos(\frac{\alpha_{21}}{2})$, $\cos\delta_{\text{CP}}$ are negative. In addition, the effective mass for the neutrinoless double beta decay is given by

$$\langle m_{ee} \rangle = |\epsilon| |\tilde{D}_{\nu_1} \cos^2 \theta_{12} \cos^2 \theta_{13} + \tilde{D}_{\nu_2} \sin^2 \theta_{12} \cos^2 \theta_{13} e^{i\alpha_{21}} + \tilde{D}_{\nu_3} \sin^2 \theta_{13} e^{-2i\delta_{\text{CP}}}|, \quad (3.22)$$

where we can compare our prediction with experimental measurements by current/future neutrinoless beta decay experiments such as KamLAND-Zen [89, 90], nEXO [91] and LEGEND [92].

4 Numerical analysis

In this section, we demonstrate the allowed space, applying χ square numerical analysis to satisfy the current neutrino oscillation data at around the each of the fixed/special points of τ , where we randomly select within the ranges of input dimensionless parameters as

$$\{\epsilon_e, \epsilon_\mu, \epsilon_\tau, \epsilon'_\tau, a_\nu, a'_\nu, b_\nu, c_\nu, \kappa_{\Sigma_{1,2}}\} \in [10^{-6} - 10^3] \quad (4.1)$$

where parameters $\{a_\ell, b_\ell, c_\ell\}$ are determined to obtain charged lepton masses. Then, we take into consideration of five reliable measured neutrino oscillation data; $(\Delta m_{\text{atm}}^2, \Delta m_{\text{sol}}^2, \sin^2 \theta_{13}, \sin^2 \theta_{23}, \sin^2 \theta_{12})$ [93], while δ_{CP} be an output parameter due to large ambiguity of experimental result in 3σ interval. For the modulus τ , we first fix it at the fixed and special points and search for the free parameters satisfying observed data. If we could not find the allowed region, we next consider τ around the fixed/special points.

4.1 NH

Here we summarize our results for the NH case at each of the fixed/special points.

4.1.1 $\tau = i$

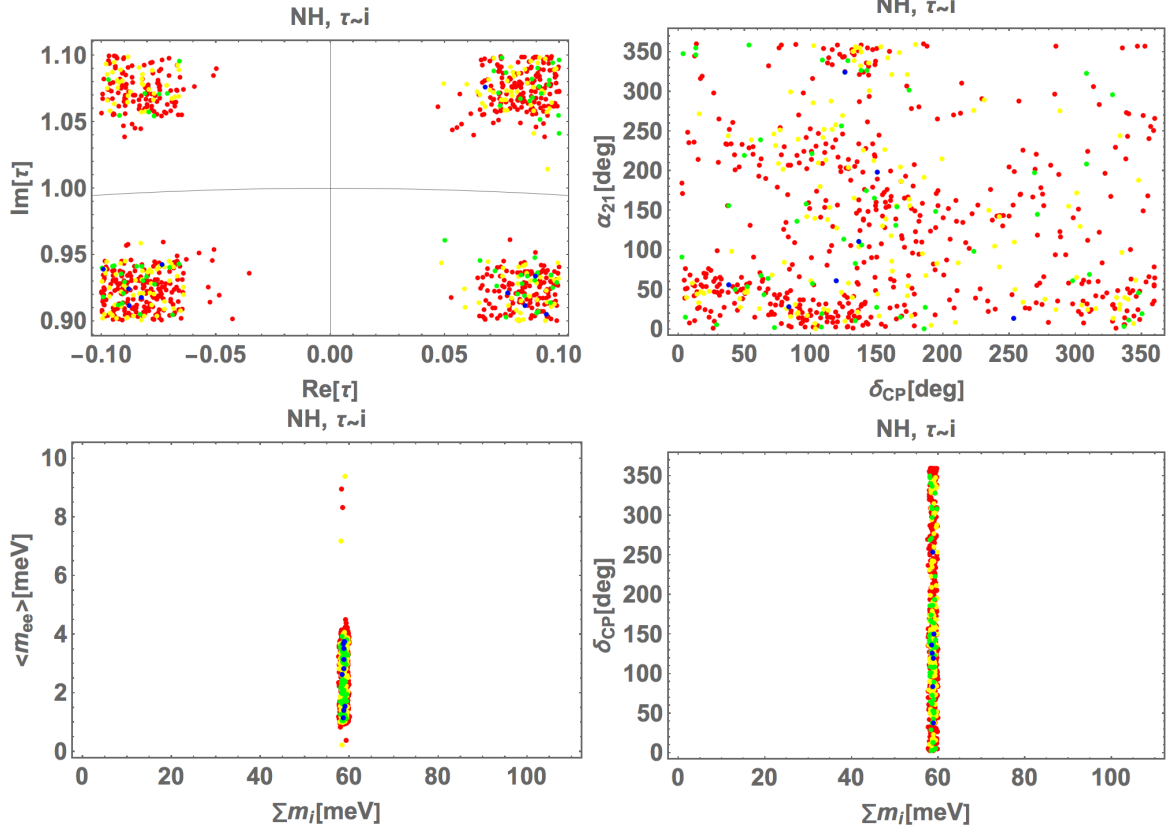


Figure 1. NH: Allowed regions in case of $\tau = i$. The colors of points indicate the χ^2 result corresponding to the level of fitting as follows; blue: within 1σ level, green: in $[1\sigma, 2\sigma]$ level, yellow: in $[2\sigma, 3\sigma]$ level, red: in $[3\sigma, 5\sigma]$ level. The color legends are the same in the figures afterwards.

In Fig. 1, we show the allowed region in case of $\tau = i$, where the left-top panel is the one for real and imaginary parts of τ , the right-top one is the correlation between Dirac CP and Majorana phases, and the left-bottom one is the correlation between the masses of total neutrinos and neutrinoless double beta decay. Each of color represents the χ^2 result corresponding to the level of fitting as follows; blue: within 1σ level, green: in $[1\sigma, 2\sigma]$ level, yellow: in $[2\sigma, 3\sigma]$ level, red: in $[3\sigma, 5\sigma]$ level. The left-top one implies that the allowed region of τ is a little deviated from the exact fixed point of $\tau = i$. The right-top one suggests that any values are allowed for both phases, even though there tend to be favored regions. The bottom ones tell us $\sum m_i \sim 60$ meV that directly comes from the experimental value, while $\langle m_{ee} \rangle$ tends to be localized at $[0-4.5]$ meV.

4.1.2 $\tau = \omega$

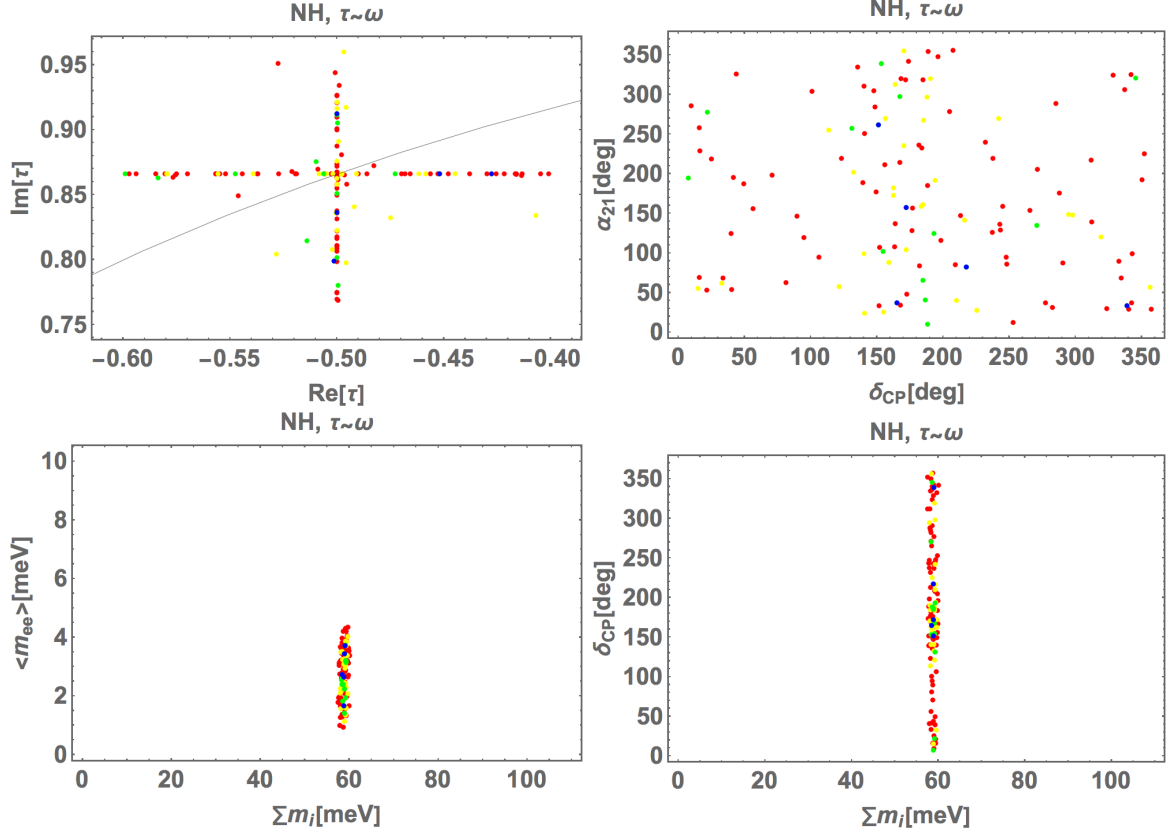


Figure 2. NH: Allowed regions in case of $\tau = \omega$.

In Fig. 2, we show the allowed region in case of $\tau = \omega$, where whole the legends are the same as the case of $\tau = i$. The left-top one implies that the allowed region of τ is at nearby $\tau = \omega$ although we would not find solutions at the exact fixed point of $\tau = \omega$. The right-top one suggests that any values are allowed for both phases and we do not find the correlation between them. The bottom ones tell us $\sum m_i \sim 60$ meV that directly comes from the experimental value, while $\langle m_{ee} \rangle$ is localized at [1–4.2] meV.

4.1.3 $\tau = -\frac{1}{2} + \frac{\sqrt{15}}{2}i$

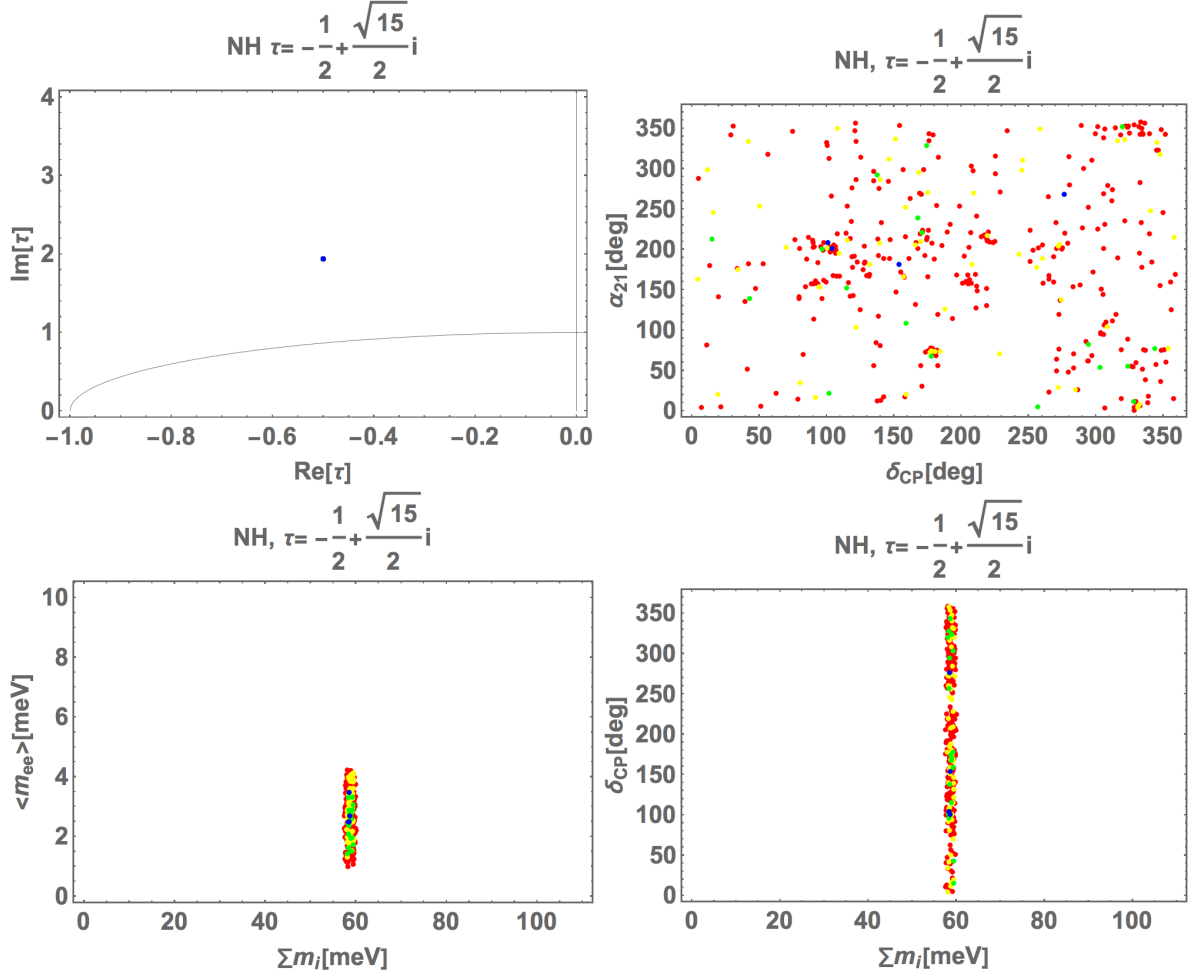


Figure 3. NH: Allowed regions in case of $\tau = -\frac{1}{2} + \frac{\sqrt{15}}{2}i$.

In Fig. 3, we show the allowed region in case of $\tau = -\frac{1}{2} + \frac{\sqrt{15}}{2}i$, where whole the legends are the same as the case of $\tau = i$. The left-top one implies that we find solutions on $\tau = -\frac{1}{2} + \frac{\sqrt{15}}{2}i$. The right-top one suggests that any values are allowed for both phases, even though there tend to be favored regions. The bottom ones tell us $\sum m_i \sim 60$ meV that directly comes from the experimental value, while $\langle m_{ee} \rangle$ is localized at [0.8–4.2] meV.

4.1.4 $\tau = \sqrt{3}i$

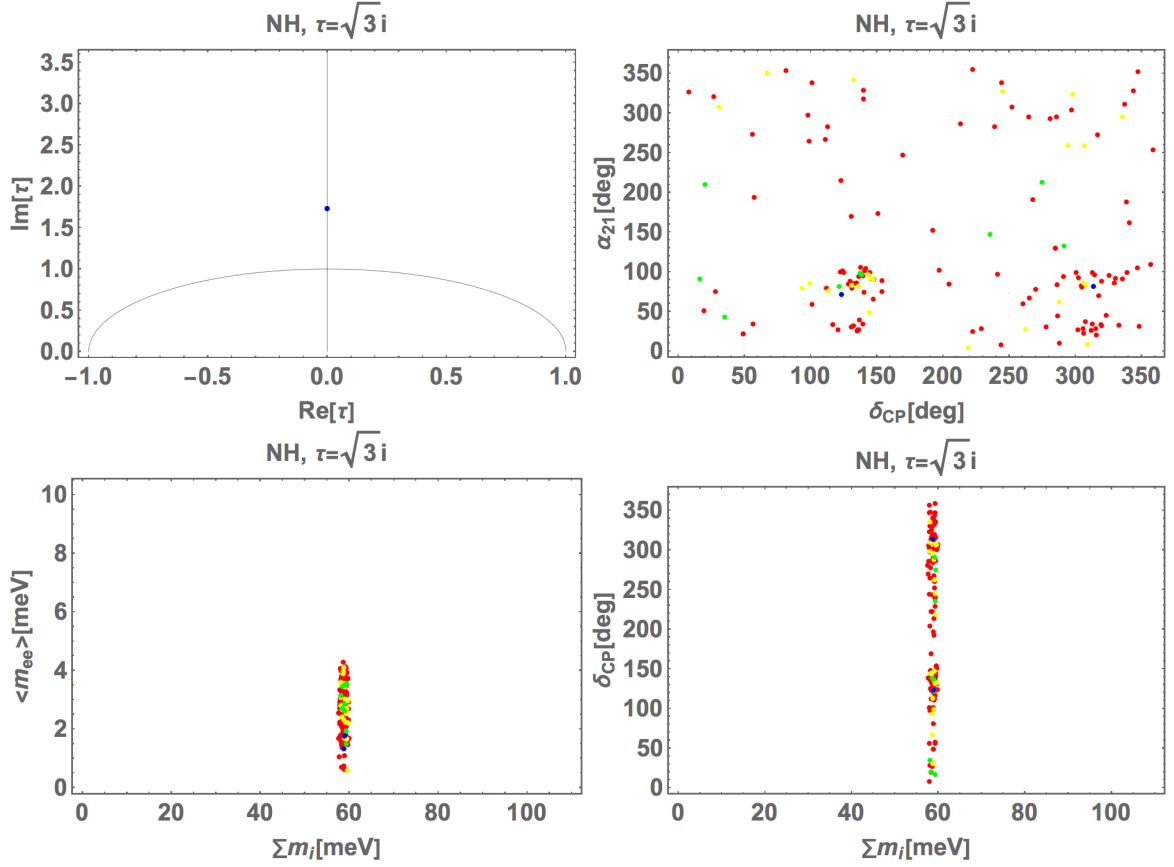


Figure 4. NH: Allowed regions in case of $\tau = \sqrt{3}i$.

In Fig. 4, we show the allowed region in case of $\tau = \sqrt{3}i$, where whole the legends are the same as the case of $\tau = i$. The left-top one implies that we find solutions on the exact special point $\tau = \sqrt{3}i$. The right-top one suggests that any values are allowed for both phases, even though there tend to be favored regions. The bottom ones tell us $\sum m_i \sim 60$ meV that directly comes from the experimental value, while $\langle m_{ee} \rangle$ is localized at $[0.5\text{--}4.2]$ meV.

4.1.5 $\tau = -\frac{1}{4} + \frac{\sqrt{15}}{4}i$

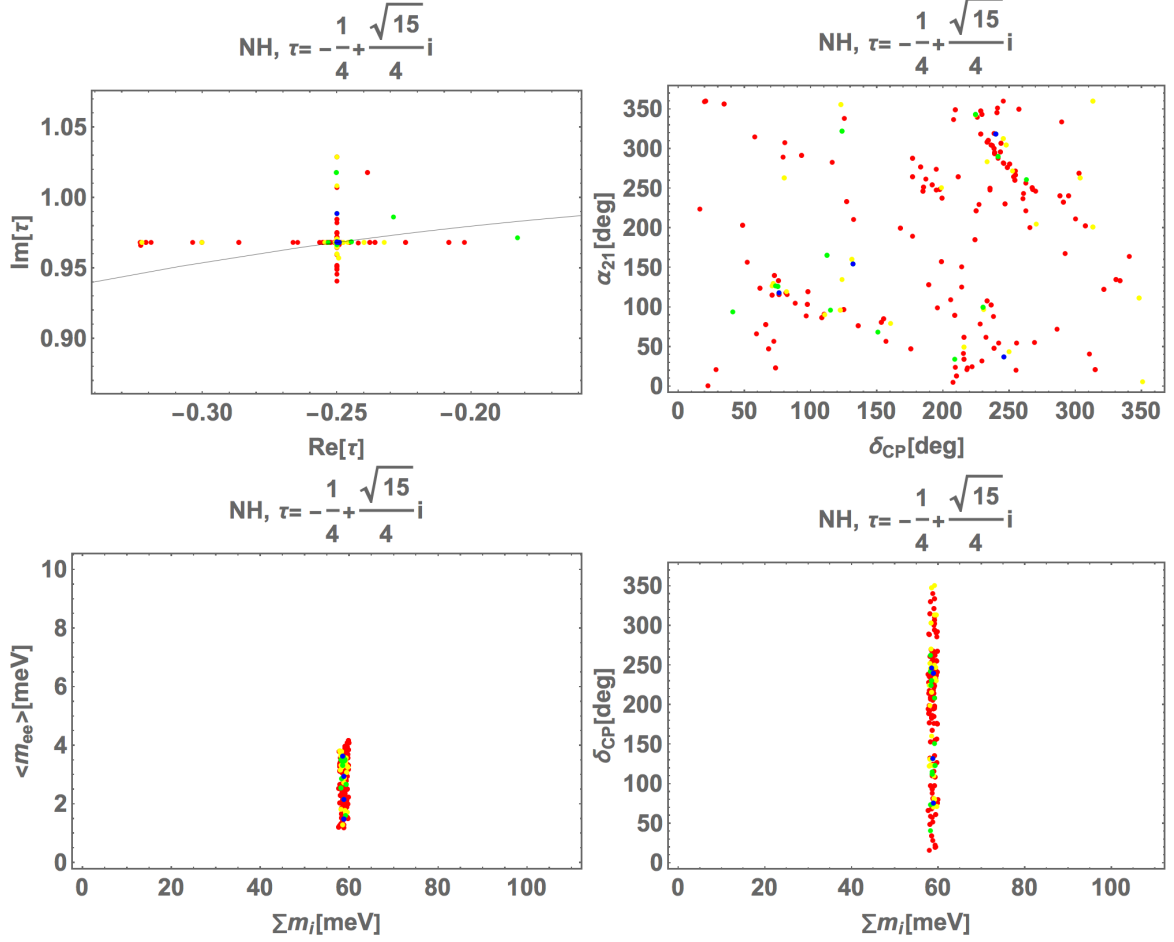


Figure 5. NH: Allowed regions in case of $\tau = -\frac{1}{4} + \frac{\sqrt{15}}{4}i$.

In Fig. 5, we show the allowed region in case of $\tau = -\frac{1}{4} + \frac{\sqrt{15}}{4}i$, where whole the legends are the same as the case of $\tau = i$. The left-top one implies that we find solutions at nearby $\tau = -\frac{1}{4} + \frac{\sqrt{15}}{4}i$. The right-top one suggests that any values are allowed for both phases, even though there exist a few localized regions. The bottom ones tell us $\sum m_i \sim 60$ meV that directly comes from the experimental value, while $\langle m_{ee} \rangle$ is localized at [1–4] meV.

4.2 IH

Here we summarize our results for the IH case at each of the fixed/special points.

4.2.1 $\tau = i$

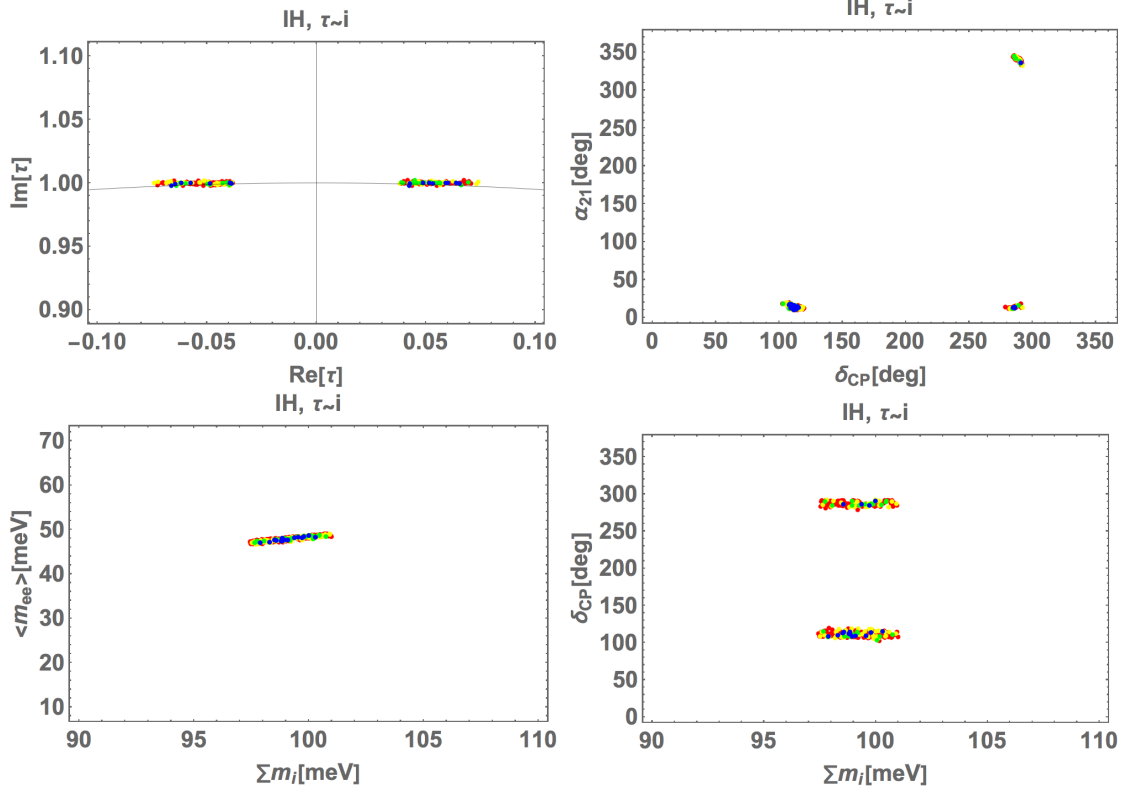


Figure 6. IH: Allowed regions in case of $\tau = i$.

In Fig. 6, we show the allowed region in case of $\tau = i$, where whole the legends are the same as the case of $\tau = i$. The left-top one implies that the allowed region of $\text{Re}[\tau]$ has a little deviation from the exact fixed point of $\tau = i$. The right-top one suggests that there exist three islands at around $[110^\circ, 10^\circ]$, $[280^\circ, 10^\circ]$, and $[280^\circ, 340^\circ]$ in terms of $[\delta_{\text{CP}}, \alpha_{21}]$. The bottom ones tell us $\sum m_i = 97 - 101$ meV that directly comes from the experimental value, while $\langle m_{ee} \rangle$ tends to be localized at 48 meV.

4.2.2 $\tau = \omega$

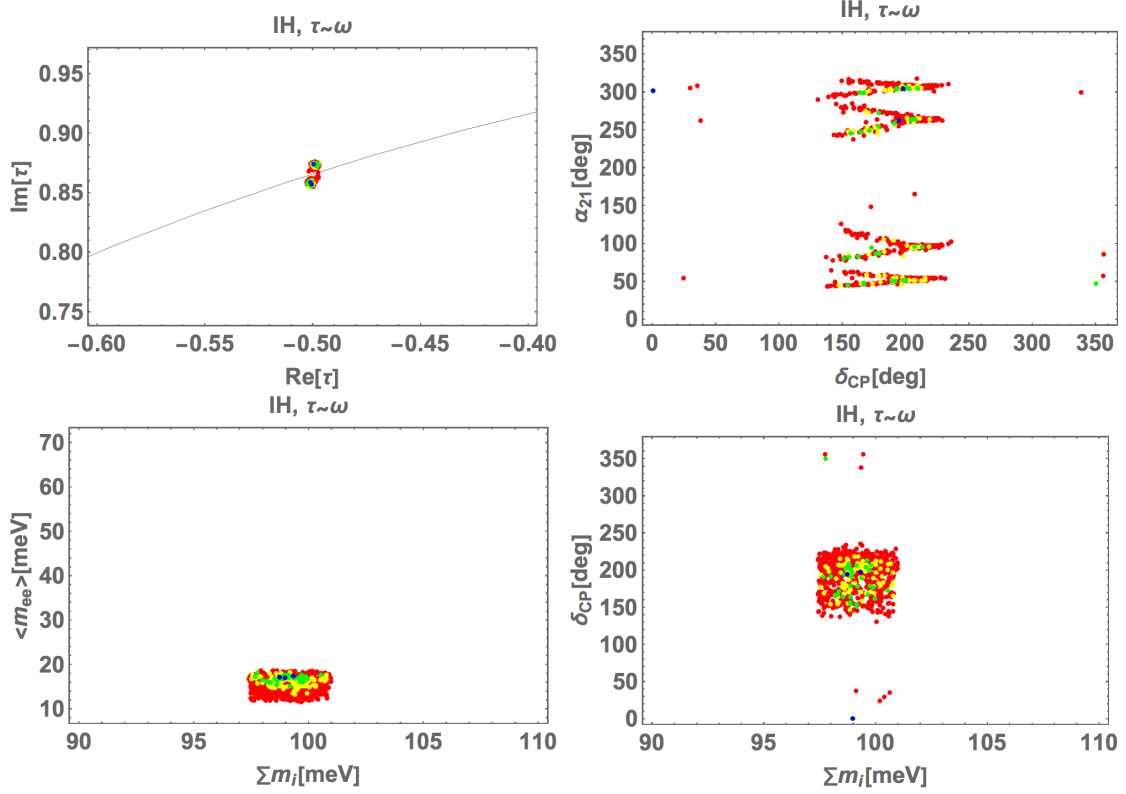


Figure 7. IH: Allowed regions in case of $\tau = \omega$.

In Fig. 7, we show the allowed region in case of $\tau = \omega$, where whole the legends are the same as the case of $\tau = i$. The left-top one implies that the allowed region of τ requires a small deviation from $\tau = \omega$. The right-top one suggests that there tends to be four islands at the common region of $140^\circ \lesssim \delta_{\text{CP}} \lesssim 240^\circ$, where α_{21} has $40^\circ - 60^\circ$, $63^\circ - 130^\circ$, $240^\circ - 280^\circ$, and $281^\circ - 310^\circ$. The bottom ones tell us $\sum m_i = 97-101$ meV that directly comes from the experimental value, while $\langle m_{ee} \rangle$ tends to be localized at 11-16 meV.

4.2.3 $\tau = -\frac{1}{2} + \frac{\sqrt{15}}{2}i$

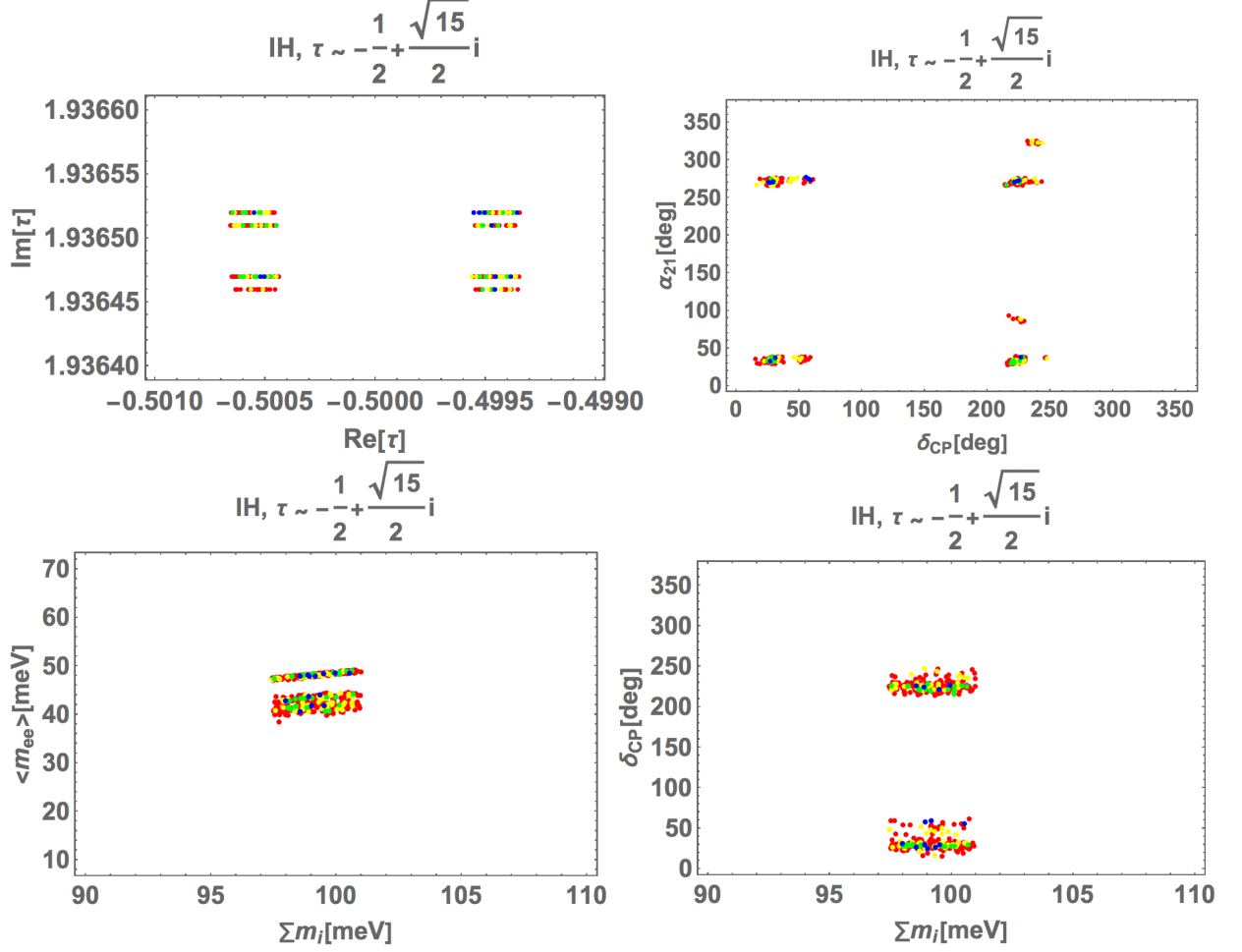


Figure 8. IH: Allowed regions in case of $\tau = -\frac{1}{2} + \frac{\sqrt{15}}{2}i$.

In Fig. 8, we show the allowed region in case of $\tau = -\frac{1}{2} + \frac{\sqrt{15}}{2}i$, where whole the legends are the same as the case of $\tau = i$. The left-top one implies that the allowed region of τ is divided by eight sectors and requires a small deviation from $\tau = -\frac{1}{2} + \frac{\sqrt{15}}{2}i$. The right-top one suggests that there exist six islands; $\alpha_{21} \simeq 30^\circ, 270^\circ$ at common region of $20^\circ \lesssim \delta_{\text{CP}} \lesssim 60^\circ$, $\alpha_{21} \simeq 30^\circ, 80^\circ, 270^\circ, 320^\circ$ at common region of $220^\circ \lesssim \delta_{\text{CP}} \lesssim 250^\circ$. The bottom ones tell us $\sum m_i = 97-101$ meV that directly comes from the experimental value, while $\langle m_{ee} \rangle$ tends to be localized at 39-44 and 46-50 meV.

4.2.4 $\tau = \sqrt{3}i$

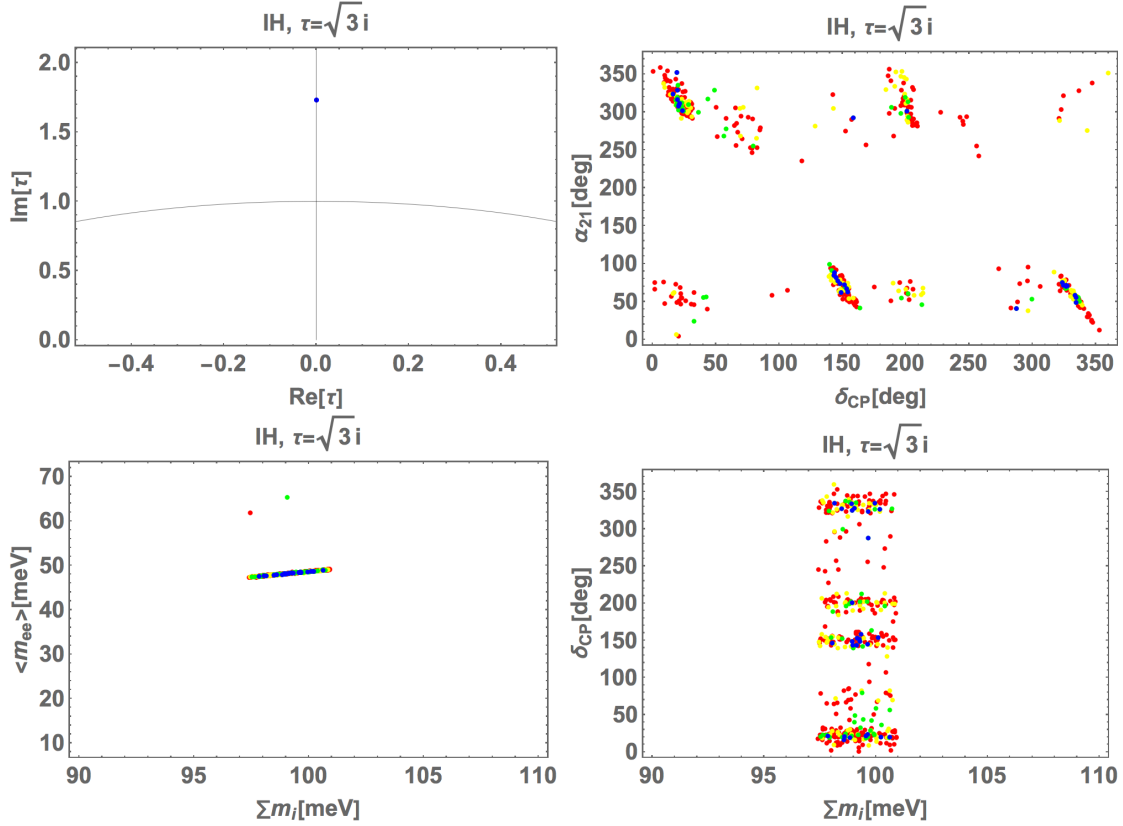


Figure 9. IH: Allowed regions in case of $\tau = \sqrt{3}i$.

In Fig. 9, we show the allowed region in case of $\tau = \sqrt{3}i$, where whole the legends are the same as the case of $\tau = i$. The left-top one implies that we find solutions at the exact special point $\tau = \sqrt{3}i$. The right-top one suggests that there exist several islands where any value is taken for δ_{CP} even though there are several dense parts. But, we have $0^\circ \lesssim \alpha_{21} \lesssim 100^\circ$ and $240^\circ \lesssim \alpha_{21} \lesssim 360^\circ$. The bottom ones tell us $\sum m_i = 97\text{-}101$ meV that directly comes from the experimental value, while $\langle m_{ee} \rangle$ tends to be localized at 46-50 meV.

4.2.5 $\tau = -\frac{1}{4} + \frac{\sqrt{15}}{4}i$

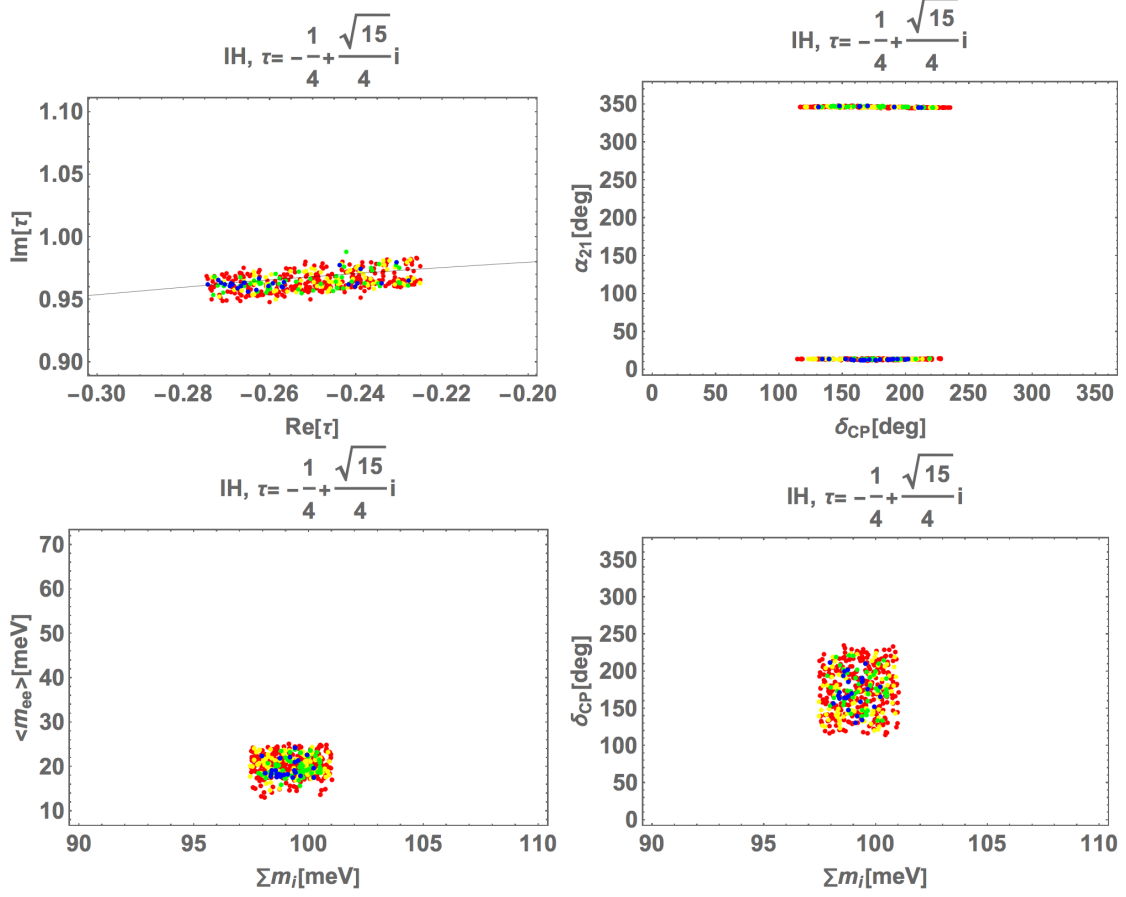


Figure 10. IH: Allowed regions in case of $\tau = -\frac{1}{4} + \frac{\sqrt{15}}{4}i$.

In Fig. 10, we show the allowed region in case of $\tau = -\frac{1}{4} + \frac{\sqrt{15}}{4}i$, where whole the legends are the same as the case of $\tau = i$. The left-top one implies that we find solutions at near by $\tau = -\frac{1}{4} + \frac{\sqrt{15}}{4}i$. The right-top one suggests $\alpha_{21} \sim 0^\circ$ and $110^\circ \lesssim \delta_{\text{CP}} \lesssim 240^\circ$. The bottom ones tell us $98 \text{ meV} \lesssim \sum m_i \lesssim 101 \text{ meV}$ that directly comes from the experimental value, while $\langle m_{ee} \rangle$ is localized at $[12\text{--}24] \text{ meV}$.

4.3 Multiple dark gauge bosons in the model

Here we briefly discuss possible phenomenology regarding dark gauge bosons from $SU(2)_H$. In the model there are three massive new neutral gauge bosons from spontaneously broken hidden $SU(2)$ gauge symmetry. Mass terms of gauge fields are obtained by kinetic terms of scalar fields

$$\begin{aligned}
 L_K = & (D_\mu H_u)^\dagger (D^\mu H_u) + (D_\mu H_d)^\dagger (D^\mu H_d) + \text{Tr}[(D_\mu \Delta)^\dagger (D^\mu \Delta)] \\
 & + (D_\mu H_X)^\dagger (D^\mu H_X) + \sum_{i=1,2} \text{Tr}[(D_\mu \Phi_i)^\dagger (D^\mu \Phi_i)].
 \end{aligned}
 \tag{4.2}$$

Covariant derivatives are written by

$$D_\mu H_u = \partial_\mu H_u - ig_2 W_\mu^i \frac{\sigma^i}{2} H_u - ig_1 \frac{1}{2} B_\mu H_u, \quad (4.3)$$

$$D_\mu H_d = \partial_\mu H_d - ig_2 W_\mu^i \frac{\sigma^i}{2} H_d + ig_1 \frac{1}{2} B_\mu H_d, \quad (4.4)$$

$$D_\mu H_X = \partial_\mu H_X - ig_X \frac{\sigma^i}{2} X_\mu^i H_X, \quad (4.5)$$

$$D_\mu \Delta = \partial_\mu \Delta - ig_H \left[\frac{\sigma^i}{2} W_{H\mu}^i, \Delta \right], \quad (4.6)$$

$$D_\mu \Phi_1 = \partial_\mu \Phi_1 - ig_2 W_\mu^i \frac{\sigma^i}{2} \Phi_1 + ig_X \frac{\sigma^i}{2} \Phi_1 X_\mu^i - ig_1 \frac{1}{2} B_\mu \Phi_1, \quad (4.7)$$

$$D_\mu \Phi_2 = \partial_\mu \Phi_2 - ig_2 W_\mu^i \frac{\sigma^i}{2} \Phi_2 + ig_X \frac{\sigma^i}{2} \Phi_1 X_\mu^i + ig_1 \frac{1}{2} B_\mu \Phi_2, \quad (4.8)$$

where $X_\mu^i (W_\mu^i)$ is the gauge associated with $SU(2)_{H(L)}$, B_μ is $U(1)_Y$ gauge field, and $\{g_1, g_2, g_X\}$ are respectively gauge couplings for $\{U(1)_Y, SU(2)_L, SU(2)_H\}$. After spontaneous gauge symmetry breaking, we obtain mass terms for gauge fields such that

$$\begin{aligned} \mathcal{L}_M^{\text{gauge}} = & \frac{1}{2} M_1^2 X_\mu^1 X^{1\mu} + \frac{1}{2} M_2^2 X_\mu^2 X^{2\mu} + \frac{1}{2} M_3^2 X_\mu^3 X^{3\mu} + \frac{1}{2} M_{\hat{Z}}^2 \hat{Z}_\mu \hat{Z}^\mu + M_W^2 W_\mu^+ W^{-\mu} \\ & + M_{\hat{Z}X^1}^2 X_\mu^1 \hat{Z}^\mu + M_{\hat{Z}X^3}^2 X_\mu^3 \hat{Z}^\mu. \end{aligned} \quad (4.9)$$

The coefficients of each term are written by

$$\begin{aligned} M_1^2 &= \frac{g_X}{4} (2v_X^2 + \bar{\kappa}^2 + \bar{\zeta}^2 + 4(v_+ - v_-)^2), \\ M_2^2 &= \frac{g_X}{4} (2v_X^2 + \bar{\kappa}^2 + \bar{\zeta}^2 + 4(v_+ + v_-)^2), \\ M_3^2 &= \frac{g_X}{4} (2v_X^2 + \bar{\kappa}^2 + \bar{\zeta}^2 + 4(v_+^2 + v_-^2)), \\ M_W^2 &= \frac{g_2^2}{4} (v^2 + \bar{\kappa}^2 + \bar{\zeta}^2), \quad M_{\hat{Z}}^2 = \frac{g_{\hat{Z}}^2}{4} (v^2 + \bar{\kappa}^2 + \bar{\zeta}^2), \\ M_{\hat{Z}X^1}^2 &= \frac{g_X g_Z}{2} (\kappa \kappa' - \zeta \zeta'), \quad M_{\hat{Z}X^3}^2 = -\frac{g_X g_Z}{4} (\kappa^2 - \kappa'^2 + \zeta^2 - \zeta'^2), \end{aligned} \quad (4.10)$$

where $v^2 = v_u^2 + v_d^2$, $\bar{\kappa}^2 = \kappa^2 + \kappa'^2$, $\bar{\zeta}^2 = \zeta^2 + \zeta'^2$, $\hat{Z}_\mu = \cos \theta_W W_\mu^3 - \sin \theta_W B_\mu$ and $g_Z = \sqrt{g_1^2 + g_2^2}$. The masses of dark gauge bosons are $M_1 \sim M_2 \sim M_3 \sim g_X v_X / 2$ for $v_X \gg \{\kappa, \kappa', \zeta, \zeta', v_+, v_-\}$. We also find that the SM Z boson mixes with X^1 and X^3 while X^2 does not mix. The mass eigenstates and eigenvalues of neutral gauge bosons can be obtained by diagonalizing 3×3 mass matrix for $\{\hat{Z}, X^1, X^3\}$. Here we omit to explicitly diagonalize the mass matrix and just require the mixings are small so that the model is safe from electroweak precision tests. For discussion we write mass eigenstate as $\{Z, Z'_1, Z'_2, Z'_3\}$ where $Z'_2 = X^2$ and Z is the SM Z boson.

By small mixing effect, two dark gauge bosons $\{Z'_1, Z'_2\}$ can decay into the SM particles directly. Their behavior is similar to dark photons that are tested by various experiments including current/future ones [94]. On the other hand, Z'_2 can decay into the SM particles through off-shell $Z'_{1,3}$, and it would be a long-lived particle. Then Z'_2 can provide an

interesting signature of the model at collider experiments. The Z'_2 can be produced through scalar mixing; for example Z'_2 can be obtained from the SM Higgs decay $h \rightarrow Z'_2 Z'_2$ if $m_h > 2m_{Z'_2}$ via scalar mixing among H_u , H_d and H_X . Produced Z'_2 would be long lived and decay mode is such as $Z'_2 \rightarrow Z'_1 Z'_3 \rightarrow f_{SM} \bar{f}_{SM} f_{SM} \bar{f}_{SM}$ where f_{SM} is a SM fermion. We thus expect long-lived particle decaying into 4 fermions, and the signal can be tested by collider experiments targeting to detect long-lived particles [95–99]. Detailed discussion of collider signals is beyond the scope of this paper and we leave it as future work.

5 Summary and discussions

We have studied flavor phenomenologies in a basis of a double covering of modular A_4 with a hidden $SU(2)$ symmetry, in which we have worked on regions at novel moduli points in addition to well-studied fixed points in $SL(2, \mathbb{Z})$ moduli space. Since these special points of $SL(2, \mathbb{Z})$ moduli space were known to be statistically favored in flux compactifications of Type IIB string theory [30], it is interesting to study the phenomenological implications of these unexplored moduli values for the lepton sector.

In our model, the neutrino masses are approximately obtained by using the seesaw mechanism due to our two additional symmetries. We have performed chi square numerical analysis for each of the fixed and special points in NH and IH and demonstrated predictions for each case. In the result we have obtained good predictions regarding $\sum m_i$ and $\langle m_{ee} \rangle$ due to model structure with T' symmetry and constrained modulus τ at fixed/special points. In case of NH, we have found that there is no deviation from all the three special points which satisfy the neutrino oscillation, while two fixed points require deviations from the exact points to find experimental solutions. Thus, there is a tendency that allowed regions of special points are rather localized than the ones of fixed points at least in focusing on the chi square within 1σ interval.⁴ In case of IH, it provides $\langle m_{ee} \rangle$ prediction around testable region and some predictions of δ_{CP} depending on different fixed/special points. While these predictions are still safe from the current constraints, they can be tested in future experiments; for example, future KamLAND-ZEN, nEXO and LEGEND for $\langle m_{ee} \rangle$, and CMB-S4 [100] for $\sum m_i$. We thus have good testability in the neutrino sector, and future measurements may find favored fixed/special point. Furthermore, we have discussed detectability at collider physics via kinetic mixings from the hidden $SU(2)$ symmetry.

Acknowledgments

The work was supported by the Fundamental Research Funds for the Central Universities (T. N.), JSPS KAKENHI Grant Numbers JP20K14477 (H. Otsuka), JP22J12877 (K. I.) and JP23H04512 (H. Otsuka).

⁴See, e.g., Ref. [31], for the mechanism to obtaining deviations from the fixed points.

Appendix

Here we summarize T' modular forms that are used in the model. The lowest weight T' modular form is weight 1 doublet written by

$$\begin{aligned} Y_2^{(1)}(\tau) &= \begin{pmatrix} y_1(\tau) & y_2(\tau) \end{pmatrix}^T, \\ y_1(\tau) &\simeq \sqrt{2}e^{\frac{7\pi}{12}i}e^{2\pi i\tau}(1 + e^{2\pi i\tau} + 2(e^{2\pi i\tau})^2 + 2(e^{2\pi i\tau})^4 + (e^{2\pi i\tau})^5 + 2(e^{2\pi i\tau})^6), \\ y_2(\tau) &\simeq \frac{1}{3} + 2e^{2\pi i\tau} + 2(e^{2\pi i\tau})^3 + 2(e^{2\pi i\tau})^4 + 4(e^{2\pi i\tau})^7 + 2(e^{2\pi i\tau})^9, \end{aligned} \quad (5.1)$$

where we applied an approximated form for the y_1 and y_2 . Higher weight modular forms are constructed by products of the lowest one.

Modular weight 2 triplet one is given by

$$\begin{aligned} Y_3^{(2)} &= \begin{pmatrix} y_1^{(2)} & y_2^{(2)} & y_3^{(2)} \end{pmatrix}^T, \\ y_1^{(2)} &= e^{\frac{\pi}{6}i}y_2^2, \quad y_2^{(2)} = e^{\frac{7\pi}{12}i}y_1y_2, \quad y_3^{(2)} = y_1^2, \end{aligned} \quad (5.2)$$

where τ dependence of modular form is omitted; also in the equations below. Modular weight 3 doublets are given by

$$\begin{aligned} Y_{2_1}^{(3)} &= \begin{pmatrix} y_1^{(3)} & y_2^{(3)} \end{pmatrix}^T, \quad Y_{2_2}^{(3)} = \begin{pmatrix} y_1'^{(3)} & y_2'^{(3)} \end{pmatrix}^T, \\ y_1^{(3)} &= 3e^{\frac{\pi}{6}i}y_1y_2^2, \quad y_2^{(3)} = \sqrt{2}e^{\frac{5\pi}{12}i}y_1^3 - e^{\frac{\pi}{6}i}y_2^3, \\ y_1'^{(3)} &= y_1^3 + (1-i)y_2^3, \quad y_2'^{(3)} = -3y_2y_1^2. \end{aligned} \quad (5.3)$$

Modular weight 4 triplet one is given by

$$\begin{aligned} Y_3^{(4)} &= \begin{pmatrix} y_1^{(4)} & y_2^{(4)} & y_3^{(4)} \end{pmatrix}^T, \\ y_1^{(4)} &= \sqrt{2}e^{\frac{7\pi}{12}i}y_1^3y_2 - e^{\frac{\pi}{3}i}y_2^4, \quad y_2^{(4)} = -y_1^4 - (1-i)y_1y_2^3, \quad y_3^{(4)} = 3e^{\frac{\pi}{6}i}y_1^2y_2^2. \end{aligned} \quad (5.4)$$

Modular weight 6 triplets are given by

$$\begin{aligned} Y_{3_1}^{(6)} &= \begin{pmatrix} y_1^{(6)} & y_2^{(6)} & y_3^{(6)} \end{pmatrix}^T, \quad Y_{3_2}^{(6)} = \begin{pmatrix} y_1'^{(6)} & y_2'^{(6)} & y_3'^{(6)} \end{pmatrix}^T, \\ y_1^{(6)} &= (4y_1^3y_2 + (1-i)y_2^4)y_1^{(2)}, \quad y_2^{(6)} = (4y_1^3y_2 + (1-i)y_2^4)y_2^{(2)}, \quad y_3^{(6)} = (4y_1^3y_2 + (1-i)y_2^4)y_3^{(2)}, \\ y_1'^{(6)} &= ((1+i)y_1^4 - 4y_1y_2^3)y_3^{(2)}, \quad y_2'^{(6)} = ((1+i)y_1^4 - 4y_1y_2^3)y_1^{(2)}, \quad y_3'^{(6)} = ((1+i)y_1^4 - 4y_1y_2^3)y_2^{(2)}. \end{aligned} \quad (5.5)$$

Modular weight 7 doublets are given by

$$\begin{aligned} Y_{2_1}^{(7)} &= \begin{pmatrix} f_1^{(7)} & f_2^{(7)} \end{pmatrix}^T, \quad Y_{2_2}^{(7)} = \begin{pmatrix} g_1^{(7)} & g_2^{(7)} \end{pmatrix}^T, \quad Y_{2'}^{(7)} = \begin{pmatrix} f_1'^{(7)} & f_2'^{(7)} \end{pmatrix}^T, \quad Y_{2''}^{(7)} = \begin{pmatrix} f_1''^{(7)} & f_2''^{(7)} \end{pmatrix}^T, \\ f_1^{(7)} &= (4y_1^3y_1 + (1-i)y_2^4)y_1^{(3)}, \quad f_2^{(7)} = (4y_1^3y_1 + (1-i)y_2^4)y_2^{(3)}, \\ g_1^{(7)} &= ((1+i)y_1^4 - 4y_1y_2^3)y_1'^{(3)}, \quad g_2^{(7)} = ((1+i)y_1^4 - 4y_1y_2^3)y_2'^{(3)}, \\ f_1'^{(7)} &= ((1+i)y_1^4 - 4y_1y_2^3)y_1^{(3)}, \quad f_2'^{(7)} = ((1+i)y_1^4 - 4y_1y_2^3)y_2^{(3)}, \\ f_1''^{(7)} &= (4y_1^3y_1 + (1-i)y_2^4)y_1'^{(3)}, \quad f_2''^{(7)} = (4y_1^3y_1 + (1-i)y_2^4)y_2'^{(3)}. \end{aligned} \quad (5.6)$$

Modular weight 10 triplets are given by

$$\begin{aligned}
Y_{3_1}^{(10)} &= \left(y_1^{(10)} \quad y_2^{(10)} \quad y_3^{(10)} \right)^T, \quad Y_{3_2}^{(10)} = \left(y_1'^{(10)} \quad y_2'^{(10)} \quad y_3'^{(10)} \right)^T, \quad Y_{3_3}^{(10)} = \left(y_1''^{(10)} \quad y_2''^{(10)} \quad y_3''^{(10)} \right)^T, \\
y_1^{(10)} &= (4y_1^3 y_2 + (1-i)y_2^4)^2 y_1^{(2)}, \quad y_2^{(10)} = (4y_1^3 y_2 + (1-i)y_2^4)^2 y_2^{(2)}, \quad y_3^{(10)} = (4y_1^3 y_2 + (1-i)y_2^4)^2 y_3^{(2)}, \\
y_1'^{(10)} &= (4y_1^3 y_2 + (1-i)y_2^4)((1+i)y_1^4 - 4y_1 y_2^3) y_3^{(2)}, \quad y_2'^{(10)} = (4y_1^3 y_2 + (1-i)y_2^4)((1+i)y_1^4 - 4y_1 y_2^3) y_1^{(2)}, \\
y_1''^{(10)} &= (4y_1^3 y_2 + (1-i)y_2^4)((1+i)y_1^4 - 4y_1 y_2^3) y_2^{(2)}, \\
y_1''^{(10)} &= ((1+i)y_1^4 - 4y_1 y_2^3)^2 y_2^{(2)}, \quad y_2''^{(10)} = ((1+i)y_1^4 - 4y_1 y_2^3)^2 y_3^{(2)}, \quad y_3''^{(10)} = ((1+i)y_1^4 - 4y_1 y_2^3)^2 y_1^{(2)}.
\end{aligned} \tag{5.7}$$

References

- [1] G. Altarelli and F. Feruglio, *Discrete Flavor Symmetries and Models of Neutrino Mixing*, *Rev. Mod. Phys.* **82** (2010) 2701 [[1002.0211](#)].
- [2] H. Ishimori, T. Kobayashi, H. Ohki, Y. Shimizu, H. Okada and M. Tanimoto, *Non-Abelian Discrete Symmetries in Particle Physics*, *Prog. Theor. Phys. Suppl.* **183** (2010) 1 [[1003.3552](#)].
- [3] T. Kobayashi, H. Ohki, H. Okada, Y. Shimizu and M. Tanimoto, *An Introduction to Non-Abelian Discrete Symmetries for Particle Physicists* (1, 2022), [10.1007/978-3-662-64679-3](#).
- [4] Y. Almuin, M.-C. Chen, V. Knapp-Pérez, S. Ramos-Sánchez, M. Ratz and S. Shukla, *Metaplectic Flavor Symmetries from Magnetized Tori*, *JHEP* **05** (2021) 078 [[2102.11286](#)].
- [5] S. Ferrara, D. Lust and S. Theisen, *Target Space Modular Invariance and Low-Energy Couplings in Orbifold Compactifications*, *Phys. Lett. B* **233** (1989) 147.
- [6] W. Lerche, D. Lust and N.P. Warner, *Duality Symmetries in $N = 2$ Landau-ginzburg Models*, *Phys. Lett. B* **231** (1989) 417.
- [7] J. Lauer, J. Mas and H.P. Nilles, *Twisted sector representations of discrete background symmetries for two-dimensional orbifolds*, *Nucl. Phys. B* **351** (1991) 353.
- [8] A. Baur, H.P. Nilles, A. Trautner and P.K.S. Vaudrevange, *Unification of Flavor, CP, and Modular Symmetries*, *Phys. Lett. B* **795** (2019) 7 [[1901.03251](#)].
- [9] A. Baur, H.P. Nilles, A. Trautner and P.K.S. Vaudrevange, *A String Theory of Flavor and \mathcal{CP}* , *Nucl. Phys. B* **947** (2019) 114737 [[1908.00805](#)].
- [10] K. Ishiguro, T. Kobayashi and H. Otsuka, *Symplectic modular symmetry in heterotic string vacua: flavor, CP, and R-symmetries*, *JHEP* **01** (2022) 020 [[2107.00487](#)].
- [11] K. Ishiguro, T. Kobayashi and H. Otsuka, *Spontaneous CP violation and symplectic modular symmetry in Calabi-Yau compactifications*, *Nucl. Phys. B* **973** (2021) 115598 [[2010.10782](#)].
- [12] T. Kobayashi, S. Nagamoto, S. Takada, S. Tamba and T.H. Tatsuishi, *Modular symmetry and non-Abelian discrete flavor symmetries in string compactification*, *Phys. Rev. D* **97** (2018) 116002 [[1804.06644](#)].
- [13] T. Kobayashi and S. Tamba, *Modular forms of finite modular subgroups from magnetized D-brane models*, *Phys. Rev. D* **99** (2019) 046001 [[1811.11384](#)].

- [14] H. Ohki, S. Uemura and R. Watanabe, *Modular flavor symmetry on a magnetized torus*, *Phys. Rev. D* **102** (2020) 085008 [[2003.04174](#)].
- [15] S. Kikuchi, T. Kobayashi, S. Takada, T.H. Tatsuishi and H. Uchida, *Revisiting modular symmetry in magnetized torus and orbifold compactifications*, *Phys. Rev. D* **102** (2020) 105010 [[2005.12642](#)].
- [16] S. Kikuchi, T. Kobayashi, H. Otsuka, S. Takada and H. Uchida, *Modular symmetry by orbifolding magnetized $T^2 \times T^2$: realization of double cover of Γ_N* , *JHEP* **11** (2020) 101 [[2007.06188](#)].
- [17] P.P. Novichkov, J.T. Penedo, S.T. Petcov and A.V. Titov, *Modular S_4 models of lepton masses and mixing*, *JHEP* **04** (2019) 005 [[1811.04933](#)].
- [18] P. Novichkov, S. Petcov and M. Tanimoto, *Trimaximal Neutrino Mixing from Modular A_4 Invariance with Residual Symmetries*, *Phys. Lett. B* **793** (2019) 247 [[1812.11289](#)].
- [19] P.P. Novichkov, J.T. Penedo, S.T. Petcov and A.V. Titov, *Modular A_5 symmetry for flavour model building*, *JHEP* **04** (2019) 174 [[1812.02158](#)].
- [20] G.-J. Ding, S.F. King, X.-G. Liu and J.-N. Lu, *Modular S_4 and A_4 symmetries and their fixed points: new predictive examples of lepton mixing*, *JHEP* **12** (2019) 030 [[1910.03460](#)].
- [21] H. Okada and M. Tanimoto, *Towards unification of quark and lepton flavors in A_4 modular invariance*, [1905.13421](#).
- [22] S.F. King and Y.-L. Zhou, *Trimaximal TM_1 mixing with two modular S_4 groups*, *Phys. Rev. D* **101** (2020) 015001 [[1908.02770](#)].
- [23] H. Okada and M. Tanimoto, *Quark and lepton flavors with common modulus τ in A_4 modular symmetry*, [2005.00775](#).
- [24] H. Okada and M. Tanimoto, *Modular invariant flavor model of A_4 and hierarchical structures at nearby fixed points*, [2009.14242](#).
- [25] H. Okada and M. Tanimoto, *Spontaneous CP violation by modulus τ in A_4 model of lepton flavors*, [2012.01688](#).
- [26] F. Feruglio, V. Gherardi, A. Romanino and A. Titov, *Modular invariant dynamics and fermion mass hierarchies around $\tau = i$* , *JHEP* **05** (2021) 242 [[2101.08718](#)].
- [27] T. Kobayashi, H. Otsuka, M. Tanimoto and K. Yamamoto, *Modular symmetry in the SMEFT*, *Phys. Rev. D* **105** (2022) 055022 [[2112.00493](#)].
- [28] T. Kobayashi, H. Otsuka, M. Tanimoto and K. Yamamoto, *Lepton flavor violation, lepton $(g - 2)_{\mu,e}$ and electron EDM in the modular symmetry*, *JHEP* **08** (2022) 013 [[2204.12325](#)].
- [29] T. Kobayashi and H. Otsuka, *Classification of discrete modular symmetries in Type IIB flux vacua*, *Phys. Rev. D* **101** (2020) 106017 [[2001.07972](#)].
- [30] K. Ishiguro, T. Kobayashi and H. Otsuka, *Landscape of Modular Symmetric Flavor Models*, *JHEP* **03** (2021) 161 [[2011.09154](#)].
- [31] K. Ishiguro, H. Okada and H. Otsuka, *Residual flavor symmetry breaking in the landscape of modular flavor models*, *JHEP* **09** (2022) 072 [[2206.04313](#)].
- [32] T. Kobayashi, T. Nomura, H. Okada and H. Otsuka, *Modular flavor models with positive modular weights: a new lepton model building*, [2310.10091](#).

- [33] T. Kobayashi, N. Omoto, Y. Shimizu, K. Takagi, M. Tanimoto and T.H. Tatsuishi, *Modular A_4 invariance and neutrino mixing*, *JHEP* **11** (2018) 196 [[1808.03012](#)].
- [34] H. Okada and M. Tanimoto, *CP violation of quarks in A_4 modular invariance*, *Phys. Lett. B* **791** (2019) 54 [[1812.09677](#)].
- [35] T. Nomura and H. Okada, *A modular A_4 symmetric model of dark matter and neutrino*, *Phys. Lett. B* **797** (2019) 134799 [[1904.03937](#)].
- [36] F.J. de Anda, S.F. King and E. Perdomo, *$SU(5)$ grand unified theory with A_4 modular symmetry*, *Phys. Rev. D* **101** (2020) 015028 [[1812.05620](#)].
- [37] T. Nomura and H. Okada, *A two loop induced neutrino mass model with modular A_4 symmetry*, [1906.03927](#).
- [38] H. Okada and Y. Orikasa, *A radiative seesaw model in modular A_4 symmetry*, [1907.13520](#).
- [39] G.-J. Ding, S.F. King and X.-G. Liu, *Modular A_4 symmetry models of neutrinos and charged leptons*, *JHEP* **09** (2019) 074 [[1907.11714](#)].
- [40] T. Nomura, H. Okada and O. Popov, *A modular A_4 symmetric scotogenic model*, *Phys. Lett. B* **803** (2020) 135294 [[1908.07457](#)].
- [41] T. Kobayashi, Y. Shimizu, K. Takagi, M. Tanimoto and T.H. Tatsuishi, *A_4 lepton flavor model and modulus stabilization from S_4 modular symmetry*, *Phys. Rev. D* **100** (2019) 115045 [[1909.05139](#)].
- [42] T. Asaka, Y. Heo, T.H. Tatsuishi and T. Yoshida, *Modular A_4 invariance and leptogenesis*, *JHEP* **01** (2020) 144 [[1909.06520](#)].
- [43] D. Zhang, *A modular A_4 symmetry realization of two-zero textures of the Majorana neutrino mass matrix*, *Nucl. Phys. B* **952** (2020) 114935 [[1910.07869](#)].
- [44] G.-J. Ding, S.F. King, X.-G. Liu and J.-N. Lu, *Modular S_4 and A_4 symmetries and their fixed points: new predictive examples of lepton mixing*, *JHEP* **12** (2019) 030 [[1910.03460](#)].
- [45] T. Kobayashi, T. Nomura and T. Shimomura, *Type II seesaw models with modular A_4 symmetry*, *Phys. Rev. D* **102** (2020) 035019 [[1912.00637](#)].
- [46] T. Nomura, H. Okada and S. Patra, *An Inverse Seesaw model with A_4 -modular symmetry*, [1912.00379](#).
- [47] X. Wang, *Lepton flavor mixing and CP violation in the minimal type-(I+II) seesaw model with a modular A_4 symmetry*, *Nucl. Phys. B* **957** (2020) 115105 [[1912.13284](#)].
- [48] H. Okada and Y. Shoji, *A radiative seesaw model with three Higgs doublets in modular A_4 symmetry*, *Nucl. Phys. B* **961** (2020) 115216 [[2003.13219](#)].
- [49] M.K. Behera, S. Singirala, S. Mishra and R. Mohanta, *A modular A_4 symmetric Scotogenic model for Neutrino mass and Dark Matter*, [2009.01806](#).
- [50] M.K. Behera, S. Mishra, S. Singirala and R. Mohanta, *Implications of A_4 modular symmetry on Neutrino mass, Mixing and Leptogenesis with Linear Seesaw*, [2007.00545](#).
- [51] T. Nomura and H. Okada, *A linear seesaw model with A_4 -modular flavor and local $U(1)_{B-L}$ symmetries*, [2007.04801](#).
- [52] T. Nomura and H. Okada, *Modular A_4 symmetric inverse seesaw model with $SU(2)_L$ multiplet fields*, [2007.15459](#).

- [53] T. Asaka, Y. Heo and T. Yoshida, *Lepton flavor model with modular A_4 symmetry in large volume limit*, *Phys. Lett. B* **811** (2020) 135956 [[2009.12120](#)].
- [54] K.I. Nagao and H. Okada, *Lepton sector in modular A_4 and gauged $U(1)_R$ symmetry*, [2010.03348](#).
- [55] D.W. Kang, J. Kim, T. Nomura and H. Okada, *Natural mass hierarchy among three heavy Majorana neutrinos for resonant leptogenesis under modular A_4 symmetry*, *JHEP* **07** (2022) 050 [[2205.08269](#)].
- [56] T. Nomura, H. Okada and H. Otsuka, *Texture zeros realization in a three-loop radiative neutrino mass model from modular A_4 symmetry*, [2309.13921](#).
- [57] P. Mishra, M.K. Behera, P. Panda, M. Ghosh and R. Mohanta, *Exploring models with modular symmetry in neutrino oscillation experiments*, *JHEP* **09** (2023) 144 [[2305.08576](#)].
- [58] R. Kumar, P. Mishra, M.K. Behera, R. Mohanta and R. Srivastava, *Predictions from scoto-seesaw with A_4 modular symmetry*, [2310.02363](#).
- [59] S. Centelles Chuliá, R. Kumar, O. Popov and R. Srivastava, *Neutrino Mass Sum Rules from Modular A_4 Symmetry*, [2308.08981](#).
- [60] M. Kashav and S. Verma, *On minimal realization of topological Lorentz structures with one-loop seesaw extensions in A_4 modular symmetry*, *JCAP* **03** (2023) 010 [[2205.06545](#)].
- [61] F. Gmeiner, R. Blumenhagen, G. Honecker, D. Lust and T. Weigand, *One in a billion: MSSM-like D-brane statistics*, *JHEP* **01** (2006) 004 [[hep-th/0510170](#)].
- [62] H. Otsuka and K. Takemoto, *$SO(32)$ heterotic standard model vacua in general Calabi-Yau compactifications*, *JHEP* **11** (2018) 034 [[1809.00838](#)].
- [63] T. Nomura and H. Okada, *Radiative interactions between new non-Abelian gauge sector and the standard model*, *Phys. Lett. B* **821** (2021) 136630 [[2104.01871](#)].
- [64] T. Nomura and H. Okada, *Radiative neutrino mass model in dark non-Abelian gauge symmetry*, *Phys. Rev. D* **105** (2022) 075010 [[2106.10451](#)].
- [65] L.M. Krauss and F. Wilczek, *Discrete Gauge Symmetry in Continuum Theories*, *Phys. Rev. Lett.* **62** (1989) 1221.
- [66] P. Ko, T. Nomura and H. Okada, *Dark matter physics in dark $SU(2)$ gauge symmetry with non-Abelian kinetic mixing*, *Phys. Rev. D* **103** (2021) 095011 [[2007.08153](#)].
- [67] C.-W. Chiang, T. Nomura and J. Tandeau, *Nonabelian Dark Matter with Resonant Annihilation*, *JHEP* **01** (2014) 183 [[1306.0882](#)].
- [68] C.-H. Chen and T. Nomura, *$SU(2)_X$ vector DM and Galactic Center gamma-ray excess*, *Phys. Lett. B* **746** (2015) 351 [[1501.07413](#)].
- [69] C.-H. Chen and T. Nomura, *Searching for vector dark matter via Higgs portal at the LHC*, *Phys. Rev. D* **93** (2016) 074019 [[1507.00886](#)].
- [70] C. Gross, O. Lebedev and Y. Mambrini, *Non-Abelian gauge fields as dark matter*, *JHEP* **08** (2015) 158 [[1505.07480](#)].
- [71] C. Boehm, M.J. Dolan and C. McCabe, *A weighty interpretation of the Galactic Centre excess*, *Phys. Rev. D* **90** (2014) 023531 [[1404.4977](#)].
- [72] T. Hambye, *Hidden vector dark matter*, *JHEP* **01** (2009) 028 [[0811.0172](#)].

- [73] S. Baek, P. Ko and W.-I. Park, *Hidden sector monopole, vector dark matter and dark radiation with Higgs portal*, *JCAP* **10** (2014) 067 [[1311.1035](#)].
- [74] V.V. Khoze and G. Ro, *Dark matter monopoles, vectors and photons*, *JHEP* **10** (2014) 061 [[1406.2291](#)].
- [75] R. Daido, S.-Y. Ho and F. Takahashi, *Hidden monopole dark matter via axion portal and its implications for direct detection searches, beam-dump experiments, and the H_0 tension*, *JHEP* **01** (2020) 185 [[1909.03627](#)].
- [76] H. Davoudiasl and I.M. Lewis, *Dark Matter from Hidden Forces*, *Phys. Rev. D* **89** (2014) 055026 [[1309.6640](#)].
- [77] A. Karam and K. Tamvakis, *Dark matter and neutrino masses from a scale-invariant multi-Higgs portal*, *Phys. Rev. D* **92** (2015) 075010 [[1508.03031](#)].
- [78] E. Witten, *An $SU(2)$ Anomaly*, *Phys. Lett. B* **117** (1982) 324.
- [79] T. Yanagida, *Horizontal Symmetry and Mass of the Top Quark*, *Phys. Rev. D* **20** (1979) 2986.
- [80] P. Minkowski, *$\mu \rightarrow e\gamma$ at a Rate of One Out of 10^9 Muon Decays?*, *Phys. Lett. B* **67** (1977) 421.
- [81] R.N. Mohapatra and G. Senjanovic, *Neutrino Mass and Spontaneous Parity Nonconservation*, *Phys. Rev. Lett.* **44** (1980) 912.
- [82] R. Blumenhagen, B. Kors, D. Lust and S. Stieberger, *Four-dimensional String Compactifications with D-Branes, Orientifolds and Fluxes*, *Phys. Rept.* **445** (2007) 1 [[hep-th/0610327](#)].
- [83] L.E. Ibanez and A.M. Uranga, *String theory and particle physics: An introduction to string phenomenology*, Cambridge University Press (2, 2012).
- [84] R. Blumenhagen, D. Lüst and S. Theisen, *Basic concepts of string theory*, Theoretical and Mathematical Physics, Springer, Heidelberg, Germany (2013), [10.1007/978-3-642-29497-6](#).
- [85] S. Gukov, C. Vafa and E. Witten, *CFT's from Calabi-Yau four folds*, *Nucl. Phys. B* **584** (2000) 69 [[hep-th/9906070](#)].
- [86] P. Betzler and E. Plauschinn, *Type IIB flux vacua and tadpole cancellation*, *Fortsch. Phys.* **67** (2019) 1900065 [[1905.08823](#)].
- [87] PARTICLE DATA GROUP collaboration, *Review of Particle Physics*, *Phys. Rev. D* **98** (2018) 030001.
- [88] Z. Maki, M. Nakagawa and S. Sakata, *Remarks on the unified model of elementary particles*, *Prog. Theor. Phys.* **28** (1962) 870.
- [89] KAMLAND-ZEN collaboration, *Search for Majorana Neutrinos near the Inverted Mass Hierarchy Rhttps://www.overleaf.com/project/63fbc595dbcf13970bf65935egion with KamLAND-Zen*, *Phys. Rev. Lett.* **117** (2016) 082503 [[1605.02889](#)].
- [90] KAMLAND-ZEN collaboration, *Search for the Majorana Nature of Neutrinos in the Inverted Mass Ordering Region with KamLAND-Zen*, *Phys. Rev. Lett.* **130** (2023) 051801 [[2203.02139](#)].
- [91] NEXO collaboration, *Sensitivity and Discovery Potential of nEXO to Neutrinoless Double Beta Decay*, *Phys. Rev. C* **97** (2018) 065503 [[1710.05075](#)].

- [92] LEGEND collaboration, *The Large Enriched Germanium Experiment for Neutrinoless Double Beta Decay (LEGEND)*, *AIP Conf. Proc.* **1894** (2017) 020027 [[1709.01980](#)].
- [93] I. Esteban, M.C. Gonzalez-Garcia, A. Hernandez-Cabezudo, M. Maltoni and T. Schwetz, *Global analysis of three-flavour neutrino oscillations: synergies and tensions in the determination of θ_{23} , δ_{CP} , and the mass ordering*, *JHEP* **01** (2019) 106 [[1811.05487](#)].
- [94] M. Bauer, P. Foldenauer and J. Jaeckel, *Hunting All the Hidden Photons*, *JHEP* **07** (2018) 094 [[1803.05466](#)].
- [95] J.L. Feng, I. Galon, F. Kling and S. Trojanowski, *ForwArd Search ExpeRiment at the LHC*, *Phys. Rev. D* **97** (2018) 035001 [[1708.09389](#)].
- [96] J.P. Chou, D. Curtin and H.J. Lubatti, *New Detectors to Explore the Lifetime Frontier*, *Phys. Lett. B* **767** (2017) 29 [[1606.06298](#)].
- [97] J.A. Evans, *Detecting Hidden Particles with MATHUSLA*, *Phys. Rev. D* **97** (2018) 055046 [[1708.08503](#)].
- [98] V.V. Gligorov, S. Knapen, M. Papucci and D.J. Robinson, *Searching for Long-lived Particles: A Compact Detector for Exotics at LHCb*, *Phys. Rev. D* **97** (2018) 015023 [[1708.09395](#)].
- [99] J.L. Feng et al., *The Forward Physics Facility at the High-Luminosity LHC*, *J. Phys. G* **50** (2023) 030501 [[2203.05090](#)].
- [100] CMB-S4 collaboration, *CMB-S4 Science Book, First Edition*, [1610.02743](#).